

Review On Laser Induced Breakdown spectroscopy: Methodology and Technical Developments

Jinto Thomas^{1,2, a)} and Hem Chandra Joshi^{1,2, b)}

¹⁾*Institute for Plasma Research, Bhat, Gandhinagar, Gujarat, India, 382428*

²⁾*Homi Bhabha National Institute, Training School Complex, Anushaktinagar, Mumbai 400094, India*

(Dated: 28 February 2023)

In this review we attempt to provide a brief account of laser induced breakdown spectroscopy (LIBS) methodology and technological developments. We also summarise various methods adopted for exploiting LIBS. Besides, a brief overview of combination of LIBS in conjunction with other methods is also given.

Keywords: LIBS, Spectroscopy, Laser plasma

CONTENTS		XIII. LIF+ LIBS	9
I. Introduction	1	XIV. Nanoparticle enhanced LIBS (NELIBS)	10
II. LIBS Methodology	2	XV. Spatial Constraint Method	11
A. Ablation types (Front ablation and Back ablation)	2	XVI. Optically trapped LIBS (OTLIBS)	11
B. Single pulse(SP)	3	XVII. Polarization Resolved LIBS (PRLIBS)	12
C. Double pulse (DP)	3	XVIII. RESONANT ENHANCED LIBS (RELIBS), RESONANT SURFACE ENHANCED LIBS (RSENILIBS)	12
III. colliding Plasma	4	XIX. Back Reflection Enhanced LIBS (BRELIBS)	12
IV. Grating induced breakdown spectroscopy (GIBS)	4	XX. Simultaneous LIBS Combination With Other Analytical Measurements	12
V. LIBS imaging/Confocal LIBS	4	A. LIBS-Raman	12
VI. Self-Absorption, Optical Thickness	5	B. LIBS-Laser Ablation- Inductively Coupled Plasma (LA-ICP)	13
VII. Self-reversal of lines	5	C. LIBS- X-Ray Fluorescence (XRF)	13
VIII. Parameter estimation	6	XXI. concluding remarks	13
A. Electron density	6	XXII. References	13
B. Electron temperature	7	I. INTRODUCTION	
IX. Local Thermodynamical Equilibrium	8		
X. Calibration free LIBS (CFLIBS)	8		
A. C Sigma graphs	8		
B. Internal reference for self-absorption correction (IRSAC)	8		
XI. Enhancement in signal/detection sensitivity	9		
A. Effect of magnetic field	9		
B. Effect of electric field	9		
C. Glow discharge LIBS (GDLIBS)	9		
D. Microwave Assisted LIBS (MALIBS)	9		
XII. Surface Enhanced LIBS (SENLIBS)	9		

I. INTRODUCTION

In the recent years laser induced breakdown spectroscopy (LIBS) has found numerous applications encompassing various field¹. Simultaneously various LIBS techniques also emerged for better exploitation and interpretation of obtained data^{2,3}. New techniques like hand held and standoff LIBS have been developed and used⁴. Optimization of time window has been pointed out in ref.⁵ Exploiting delayed emission for LIBS indentation has also been suggested⁶.

From time to time review articles covering various aspects of LIBS have come up in the literature⁷⁻¹⁸. However they are focused on particular aspect or technique

^{a)}Electronic mail: jinto@ipr.res.in

^{b)}Electronic mail: hem'sup@yahoo.co.uk

e.g. study of uranium containing compounds¹⁹, plasma facing components^{20,21}, LIBS imaging²² element analysis of industrial materials²³ and data analysis²⁴, nano particles in LIBS^{25,26}, industrial applications²⁷, underwater applications²⁸, food analysis²⁹, optical diagnostics and laser produced plasma^{30,31}, cancer diagnostics and classification³², rapid CPVID detection¹ (Scientific reports 12, 2022, 1614) aerosol analysis³³ and geological samples³⁴. Hand held and portable LIBS technique is reviewed in reference⁴. Technique used in LIBS quantification have also progressed³⁵ in the past. Ultra sensitive and multianalyte analysis of plasma plumes using laser induced fluorescence (LIF) has been reviewed in a recent article³⁶. Combination of other techniques e.g. FTIR, Raman and Hyper spectral imaging (HI) have been elucidated to gather detailed spatial information^{37,38,39,40} Hybrid LIBS-Raman-LIF been discussed in a recent review⁴¹.

Despite these reports, efforts are continuously emerging to extend the LIBS detection range and its application in various platforms e.g. study of deposition on the tokamak first wall components⁴², analysis of hydrogen isotopes³⁰ hardness estimation etc. In this short review we attempt to briefly sketch salient features associated with LIBS which encompass phenomenological aspects to emerging applications and recent technical developments. Some new features e.g. colliding plasma, application of self-reversal in estimating isotopic abundance, filament induced LIBS and grating induced LIBS are also briefly covered. The overall goal of this article to provide with first hand information to the LIBS community. We describe it in the following sections

II. LIBS METHODOLOGY

When a substance is irradiated with a high power laser, the material is heated and results in melt which finally forms a plasma plume which consists of atom, ions and electrons. The mechanism and timescales of ablation process and subsequent plasma formation for short (fs) and long (ns) pulses are demonstrated in Fig 1. In ns-LIBS, at initial times in plasma formation the primary mechanisms are thermal vaporization and non-thermal evaporation whereas in case of fs LIBS, thermal evaporation occurs after Coulomb explosion, electron-ion energy transfer and heating of lattice by electrons which are followed by thermal vaporization. However, at later stages in case of ns LIBS, plasma reflection, absorption and reflection can occur whereas later stages for both ns and fs LIBS comprise of plasma-ambient interaction, shock wave propagation and confinement. Finally both are characterized by LIBS regime followed by plume condensation and particle ejection. Plume hydrodynamics has been found to play an important role in molecular and nano-cluster formation. In the early stages, shock wave at the edge has been found to hinder molecular formation which takes place only after the shock wave

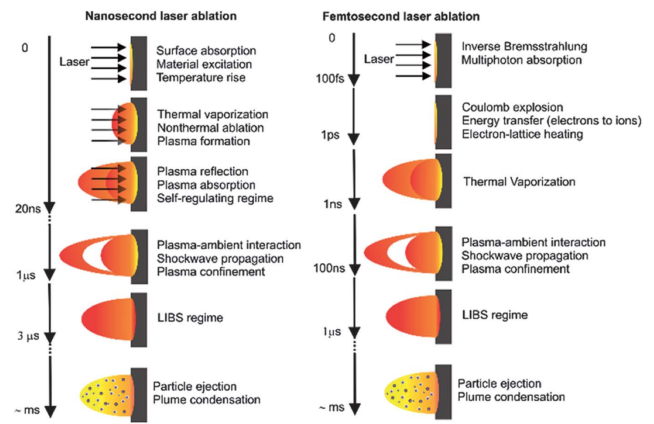


FIG. 1. Approximate time scales of nanosecond and femtosecond energy absorption and laser ablation along with various processes happening during and after the laser pulse (adapted with permission from reference⁴³).

collapse⁴⁴. Regarding expansion behavior, a systematic study is carried out for fs, ps and ns ablations⁴⁵. Differences in the propagation of the plume are observed for these three cases. For forward ablation of nickel thin film, in case of fs ablation, linear expansion is noticed for low background pressures which eventually shows shock wave like expansion at higher background pressures. For ps ablation, blast wave model describes the expansion at low pressures but a drag model appears appropriate for higher pressures. For fs ablation, effect of laser fluence on the emission characteristics in ultrafast laser produced copper was reported by Anoop et.al⁴⁶. At low to moderate fluences, neutral emission dominates but at higher fluences, ionic emission is predominant. Fast and slow components are also noticed in case of Zn (I) 481 nm emission in ultrafast laser produced zinc plasma which are ascribed to neutral and recombination contributions to the emission⁴⁷.

A. Ablation types (Front ablation and Back ablation)

In LIBS, basically the material can be ablated in three configurations viz. front, back and non-orthogonal ablation. Front and rear ablation geometries for thin film target are shown in Fig 2 and Fig 3. When laser is incident from the front side, it is termed as front ablation. On the other hand, when the laser is incident from backside, it is named as back or rear ablation. Notable differences in plume expansion geometry, composition of the plume and plume velocity are noticed. Higher velocity is obtained in case of front ablation as compared to the rear ablation⁴⁸. Moreover, spherical shock wave front is observed for both the cases, however, front side ablation has been found to have more excited state species as compared to rear ablation⁴⁹. Further, neutral species dominate in the rear ablation geometry⁵⁰.

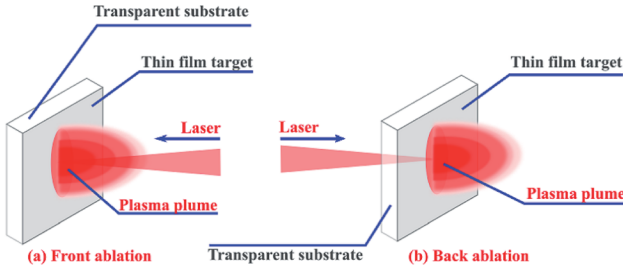


FIG. 2. Schematic diagram of laser produced plasma plume of thin film deposited on a transparent substrate in front ablation (FA) and back ablation (BA) geometries (adapted with permission from reference⁵⁰).

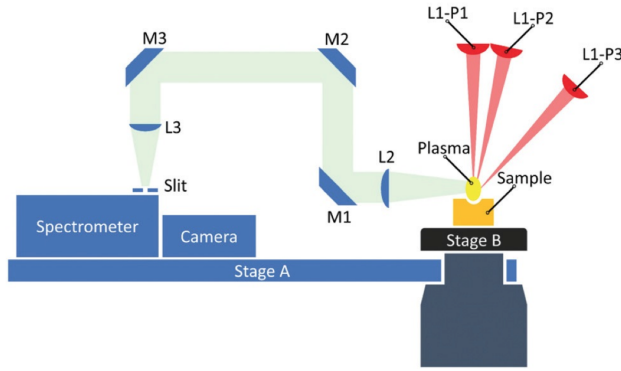


FIG. 3. Schematic diagram of the tomographic system for demonstrating the effect of non-orthogonal ablation (adapted with permission from reference⁵¹).

Besides these two geometries, laser ablation for different incident angles of laser beam has also been studied. Non orthogonal ablation has been found to increase inhomogeneity. It has been found to be composed of two parts; one following the ablation pulse and the other expanding along the sample normal. Moreover, the temporal evolution of the plasma, ionic and neutral emission and electron density and temperature have been found to exhibit similar trends.

B. Single pulse(SP)

In most of the LIBS experiments single pulsed laser is used for ablation. The pulse of the laser can vary from femtosecond to microsecond time⁵². Enhancement in intensity with long ns pulses has been reported in submerged solids⁵². Moreover, long ns pulses have been found to produce plasma with stronger emission and longer lifetime as compared to LIBS using short (35 ns) pulses. Figure 4 shows the LIBS studies using short (35 ns) and long (180 ns) laser pulses for copper⁵³.

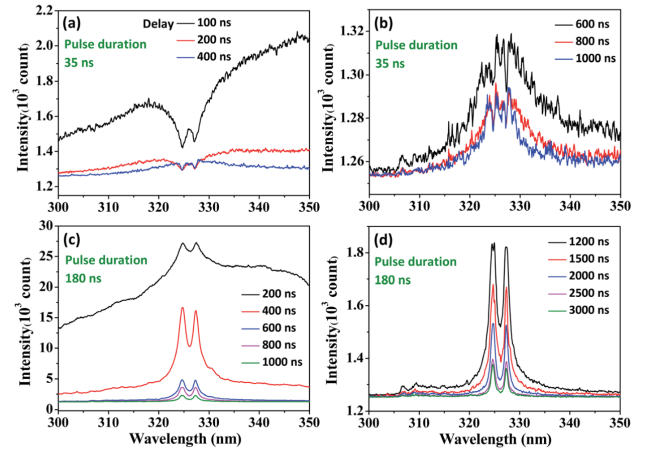


FIG. 4. Typical LIBS spectra of the atomic lines of Cu at varied delay times obtained at two pulse durations of 35ns (a and b) and 180 ns (c and d) (adapted with permission from reference⁵³).

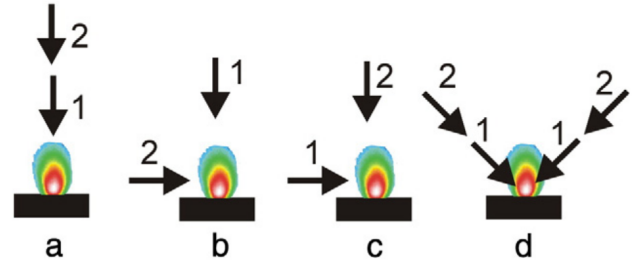


FIG. 5. Various DP configurations (a) Collinear DP, (b) Orthogonal reheating DP (c) orthogonal pre ablation DP and (d) dual pulsed cross beam (adapted with permission from reference⁵⁴).

C. Double pulse (DP)

Double pulse (DP) LIBS has been found to enhance intensity of the atomic/ionic lines depending on inter pulse delay⁵⁵. A simple schematic of various configurations of DP LIBS is shown in Fig 5. The DP configuration can be collinear (a), orthogonal reheating (b) orthogonal pre ablation (c) or dual laser cross beam (d). Further, DP LIBS can also have different configurations depending on lasers. It can have nanosecond + nanosecond (ns+ns), femtosecond+ femtosecond (fs+fs) femtosecond+ nanosecond (fs+ns) or nanosecond+ femtosecond (ns+fs) configurations. It has been found that the spectral intensity of copper plasma is higher in case of the configuration fs+ns⁵⁵. The plasma temperature has been found to be lower whereas electron density is higher. It has been suggested that the second pulse re-excites the plasma resulting in enhanced spectral intensity. Intensity enhancement has also been reported for orthogonal fs+fs DP LIBS⁵⁶ and is projected for LIBS imaging with

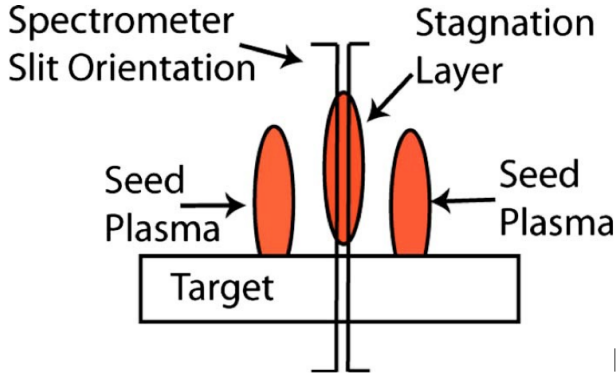


FIG. 6. Illustration of the orientation of the spectrometer slit with respect to the stagnation layer. This arrangement can provide one dimensional spatial resolution normal to the target along the stagnation layer (adapted with permission from reference⁵⁹).

better spatial resolution and spectro-chemical sensitivity. Effect of inverse Bremsstrahlung is reported for DP LIBS⁵⁷. In a recent work, effect of DP ablation on the emission characteristics of plasma has been theoretically treated using hydrodynamic model⁵⁸. Enhancement in intensity is attributed to two mechanisms viz plasma-plasma coupling effect and pressure effect.

III. COLLIDING PLASMA

When two laser produced plasmas (known as seed plasmas) are made to interact, an interaction zone is formed. This interaction zone is characterized by a stagnation layer. Colliding plasma schemes are useful in understanding plasma screening effects in fusion devices⁶⁰. A simple setup for colliding plasma is shown in Fig 6. The spectrometer slit is aligned along the propagation of stagnation layer. However, the properties of the stagnation region depend on the relative orientation of the targets from which seed plasma are formed. Two widely used target configurations- plane and wedge shaped for plasma collision studies.

Further, collisionality parameter ($\zeta = D/\lambda_{ii}$) is defined to represent various scenarios where D is the separation between the two seed plasmas and λ_{ii} is ion-ion mean free path defined by

$$\lambda_{ii}(1 \rightarrow 2) = \frac{4\pi\epsilon_0^2 m_i^2 v_{12}^4}{e^4 Z^4 n_i \ln \Delta_{12}} \quad (1)$$

Collisionality parameter $\zeta > 1$ indicates soft stagnation or interpenetration of the plumes species of seed plasma whereas $\zeta < 1$ indicates the condition of hard stagnation (in this case collisions among the seed plasmas will dominate and result in heated plasma. As mean free path is highly dependent on V_{12} and to a lesser extent

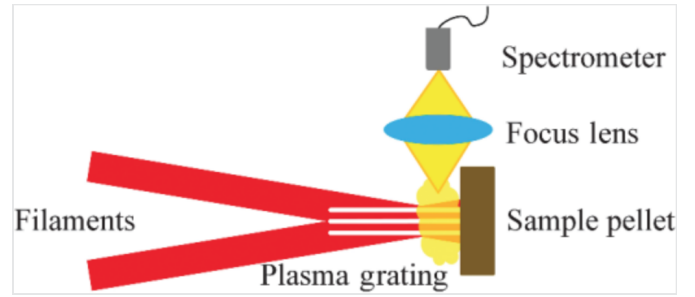


FIG. 7. Experimental schematic diagram of GIBS (adapted with permission from reference⁶⁷).

on m_i , the collisionality condition can be engineered by the orientation of the seed plasmas with respect to each other and target material. Further, the colliding plasma can be homogeneous or heterogeneous. If the seed plasmas are from the same element, it is called homogeneous whereas seed plasmas from different elements termed as heterogeneous. Signatures of enhanced neutral emission and molecular formation have been reported for the interaction zone⁶¹. Moreover properties of interaction zone are also modulated in the presence of magnetic field⁶². By observing the lines corresponding to trace elements, Tiwari et al⁶³ showed that sensitivity can be optimized using colliding plasma in the presence of the magnetic field. In an other recent study Delaney et al⁶⁴ studied the properties of stagnation layer formed in case of laterally colliding plasmas and annular plasmas and found that limit of detection (LOD) can be improved in case of colliding plasmas⁶⁴.

IV. GRATING INDUCED BREAKDOWN SPECTROSCOPY (GIBS)

In conventional ns-LIBS technique, plasma shielding affects its reproducibility, repeatability and signal to noise ratio. Interestingly in filament induced breakdown spectroscopy (FIBG), remarkable property of the filaments to travel long distances independently of the diffraction limit makes it suitable for long range operation⁶⁵. In case of FIBG, the problem of shielding is overcome but the power density profile is limited. These problems can be countered in plasma grating induced breakdown spectroscopy (GIBS)⁶⁶. A simple illustration of FIBG is shown in Fig 7. Fig 8 shows improvement in intensity of Si 288.2 nm line with GIBS.

V. LIBS IMAGING/CONFOCAL LIBS

Spatially resolved LIBS imaging has attracted considerable interest because of its importance in revealing elemental distribution in the sample. For improving lateral resolution in LIBS imaging techniques e.g. micro-LIBS, fs-LIBS and near field enhanced atomic emission spec-

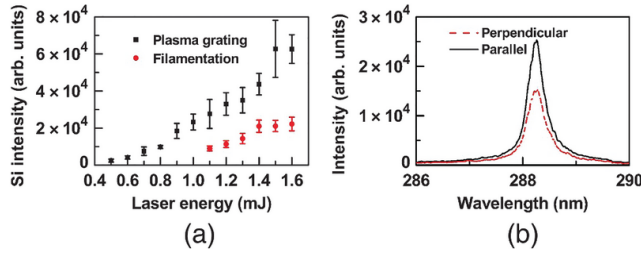


FIG. 8. (a) Intensity of the Si 288.2 nm line as a function of the laser pulse energy detected with the FIBS and GIBS systems. (b) Intensity of the Si 288.2 nm line obtained by interaction of two beams with different polarizations. Intensity enhancement is evident in case of GIBS which also depends on polarization (adapted with permission from reference⁶⁷).

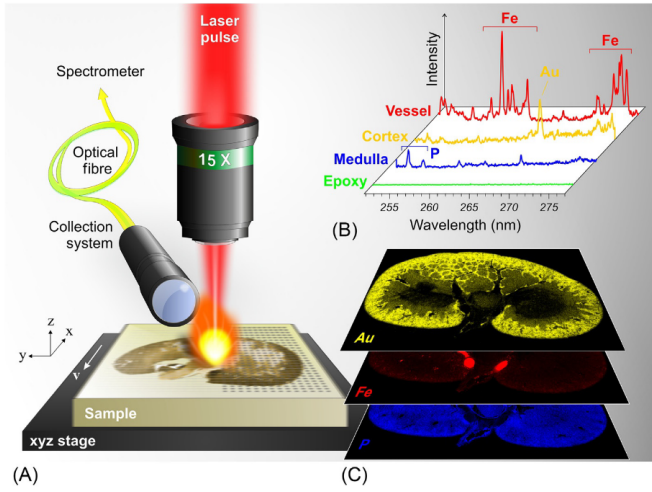


FIG. 9. General protocol for LIBS imaging (A) Schematic view of the LIBS imaging setup with main components: the microscope objective is used to focus the laser pulse, the motorized platform for moving the sample, and the detection system connected to a spectrometer via an optical fiber. (B) Examples of single-shot emission spectra in the spectral range between 250 and 280 nm. (C) Sample relative-abundance images of Au (yellow), Fe (red), and P (blue) represented using false color scales. (adapted with permission from reference⁶⁶)

troscopy have been proposed⁶⁶. Figure 9 demonstrates the general protocol for LIBS imaging whereas fig 10 shows confocal LIBS imaging setup.

VI. SELF-ABSORPTION, OPTICAL THICKNESS

LIBS based spectro-chemical analysis based on relation between the observed intensity of an emission line and analyte concentration and from analytical point of view a linear relationship is desired. However, If optical thickness is large, part of the emitted radiation will be reabsorbed by the same species which is termed as self-absorption⁶⁹. Self-absorption coefficient (SA) is de-

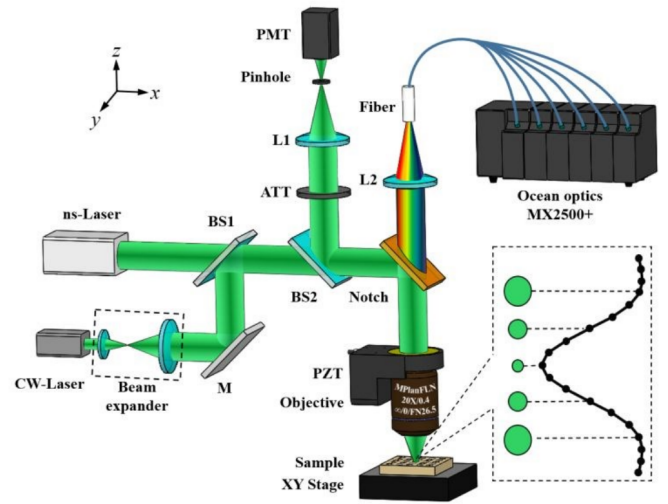


FIG. 10. Schematic of Confocal LIBS microscopy. The beam emitted from continuous-wave (CW) laser passes through a beam expander and beam splitters BS1 and BS2, and then is focused onto the sample by an objective. The reflected light transmits along the original light path and is reflected by the BS2, and then is finally detected by a photomultiplier tube (PMT) (adapted with permission from reference⁶⁸).

defined as the ratio of the actual intensity of an emission line to the theoretical intensity⁷⁰. Cases of self-absorption in case of homogeneous as well as inhomogeneous plasm are well described by Fatemeh Rezaei et al⁶⁹. A simplest check to ensure that the plasma is thin is to check the ratio of intensities of two lines which originate from same upper energy level or with upper energy levels with a small difference and if the following relation holds, it can be assumed to be optically thin.

$$\frac{I_1}{I_2} = \frac{g_1 A_1 \lambda_2}{g_2 A_2 \lambda_1} \quad (2)$$

where I, g, A, λ with subscripts are the intensities, gaunt factor, transition probabilities and wavelengths respectively of the lines 1 and 2 under consideration. Another way to is to estimate spectral absorption at the center of a line originating in levels i and j and can be given by

$$k_{ji}(\lambda_0) = 8.85 \times 10^{-13} f_{ji} \lambda_0^2 n_i P_{ji}(\lambda_0) \quad (3)$$

where $k_{ji} (cm^{-1})$ is absorption coefficient, f_{ji} is the absorption oscillator strength, λ_0 is the wavelength and $P_{ji}(\lambda_0)$ is normalized line profile at the center. For Lorentzian profile $P_{ji}(\lambda_0) = 1/(\pi \Delta \lambda_{1/2})$.

VII. SELF-REVERSAL OF LINES

Self reversal results when the emission from the hot center is absorbed by the species present at cooler periphery or due to plasma inhomogeneity⁷¹ as shown in figure 11. The emitted line shows dip at the peak due to absorption of the emitted line at rather hotter plasma

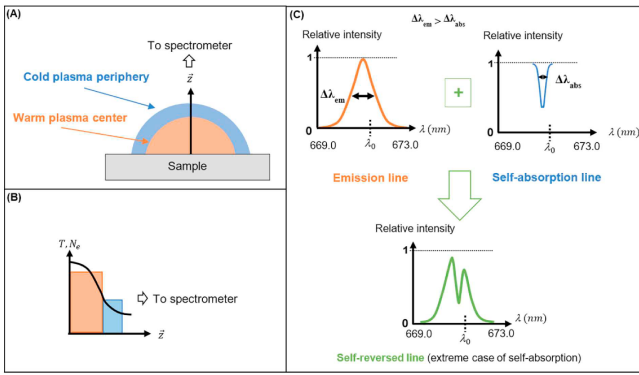


FIG. 11. Figure (a, b) depicts how self-reversal can take place; (c,d) shows self-reversal in 670.8 nm resonance line of Lithium (Li I) (adapted with permission from reference⁷¹).

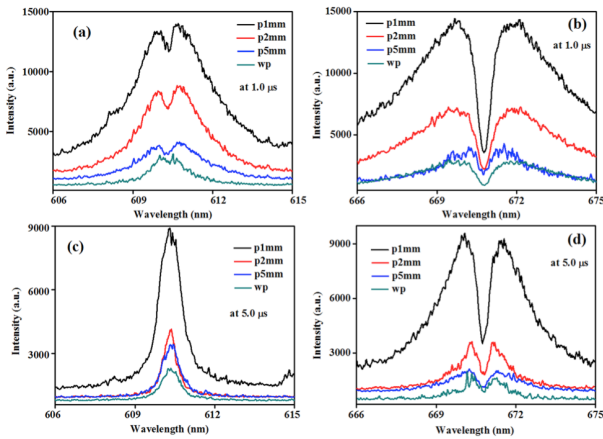


FIG. 12. Self-reversal in Lithium 670.8 nm and 610.3 nm lines in a confined geometry. More pronounced self-reversal is clearly evident for 670.8 nm resonance line (adapted with permission from reference⁷²).

center. A number of studies reported the presence of self-reversed lines under different plasma environments^{71–75}. Strong self-reversal in Li 670.8 line is noticed when LIBS was performed in a confined geometry as shown in figure 12. Moreover, it is dependent on the distance of the plate used to confine the plasma and time delay⁷². Strong self-reversal was also reported in laser produced plasma for Ba ionic line⁷³. Shock waves during breakdown had also been considered to play an important role in generating plasma inhomogeneities⁷⁴. Laser induced fluorescence (LIF) of laser ablated filaments has been found to reduce the self-reversal features in the spectral profiles⁷⁵.

Self-reversal of lines in LIBS which was considered to be unwanted, appears to be boon in disguise. Estimation of isotopic abundance in case of lithium isotopes has been projected by exploiting the narrow (less effected by line broadening processes) self-reversed profile⁷¹. With further optimization and analysis of self-reversed lines, better quantitative estimate of isotopic abundance is ex-

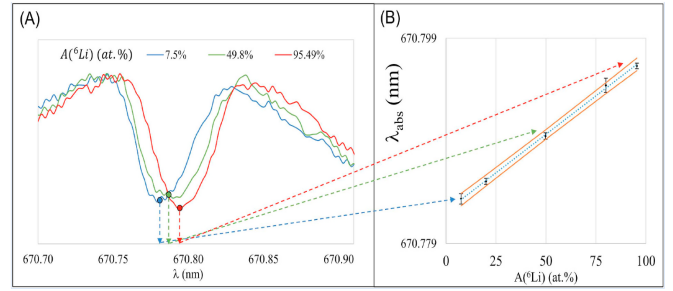


FIG. 13. Self reversal demonstrating Li isotopic dependence (adapted with permission from reference⁷¹).

pected. Figure 13 shows the isotopic dependence of self reversal profiles for lithium 670.8nm resonance line.

VIII. PARAMETER ESTIMATION

The estimation of two important parameters viz electron density and electron temperature is important in understanding the plasma plume behavior as well as estimation of elemental composition.

A. Electron density

Electron density is mainly estimated from the Stark broadening of the lines and is well established in literature and will not be detailed in the present article. However, in some cases Stark parameters of certain lines are not available and hence need to be estimated. One of the adopted methods is to use an alloy with other metal with known Stark parameters and from the obtained density extract the unknown Stark parameters⁷⁶. In another study Aragon et al. used fused glass samples to extract the Stark parameters for FeII and Ni II and Ti II with improved line to background ratios^{77,78}. In some cases, these parameters are estimated from H_α line due to the presence of trace amount of water. In case of nickel Stark parameters are estimated from the density obtained from H_α line^{79,80}. Parameters for some lines of tungsten were estimated by using CII line (426.7 nm) in tungsten carbide plasma⁸¹. Cross calibration in a multi element plasma was also used to extract these parameters⁸². Stark widths for UI and UII were estimated from the O I 799.19 nm line present as surface impurity in a uranium metal target³¹. Stark broadening coefficients for Tantalum lines were extracted using extended C-sigma method⁸³ from the information of Stark broadening coefficient for a known line. However, these methods either may suffer from the interference from the presence of more elements on the plasma or the lines from the tracer impurities may be weak to provide sufficient intensity. Moreover presence of hydrogen, at low pressures presence of trace amount of water can give H_α

line but may have low intensity. At the same time at higher air pressure (higher water content is expected), water is likely to contaminate the plasma as well as affect the plasma properties. From H_α , we can estimate Stark parameters of any element.

The spectral emission from LPP plasma are broadened due to various mechanisms, such as Stark, Doppler, van der Waals etc.⁸⁴. The line shape of emission from LPP plasma varies depending on the broadening mechanisms. A Lorentzian profile is expected for the collisional broadening process such as Stark and van der Waal broadening. whereas Doppler broadening results in a Gaussian profile. Some times more than one mechanism results in the broadening and hence the lines shape will be a convolution of different profiles as discussed in details by Griem⁸⁴

In LPP, three primary mechanisms can contribute to the spectral line shape; Doppler, Stark and instrumental. FWHM due to Doppler broadening can be estimated by

$$\Delta\lambda = 7.2 \times 10^{-7} \lambda_0 \sqrt{\frac{T_e}{M}} \quad (4)$$

In case of LIBS, the main broadening mechanism is considered as Stark broadening as due to low temperature, contribution from Doppler is very small. The Stark width is given by

$$\Delta\lambda_{1/2} = 2W\left(\frac{n_e}{10^{16}}\right)A^0 \quad (5)$$

Though the Stark broadening contribution is dominant in LPP plasma, the Doppler broadening may come significant at LPP emission of a plume expanding into a low background pressure and at a later time where the plasma density is not high. Assuming instrumental width as Lorentzian, the actual Stark width can be deducted by subtracting the instrumental width from the fitted Lorentzian width. Besides, Stark broadening, Laser Thomson scattering and interferometry can also be used to estimate electron density in laser produced plasmas^{85,86}. It has been described in an earlier review article also⁸⁷.

B. Electron temperature

The estimation of plasma parameter using the OES is based on the Boltzmann and Saha equation. Boltzmann equation relates the ratio of population densities N_j^z of excited energy levels and the number density N^z with temperature T as

$$\frac{N_j^z}{N^z} = \frac{g_j^z \exp\left(\frac{-E_j^z}{kT}\right)}{U^z(T)} \quad (6)$$

where z represents the ionization stages, E_j^z and g_j^z are the respective energy and degeneracy of the specified level, $U^z(T)$ is the partition function. The Saha equation relates electron density (N_e) and temperature with,

population density of different states z and $z - 1$ as follows

$$\frac{N_e N^z}{N^{z-1}} = \frac{2U^z(T)}{U^{z-1}(T)} \left(\frac{2\pi mkT}{h^2}\right)^{3/2} \exp\left[\frac{-(E_\infty^{z-1} - \Delta E_\infty^{z-1})}{kT}\right] \quad (7)$$

where E_∞^{z-1} is the ionisation energy of species in charge state of $z-1$, ΔE_∞^{z-1} is the correction in ionization energy due to the plasma interaction, h is Planck's constant ($6.626 \times 10^{-34} J.s$), m is the mass of the electron ($9.109 \times 10^{-31} Kg$). All these parameters for most of the species are well known and available in data bases like NIST. The applicability of these equations largely depends on the validity of LTE conditions of plasma described in section IX.

Electron temperature can be estimated using the ratio of emission intensities of spectral lines of the same species and charge states using the Boltzman equation (Equation (6)). Estimation of temperature is normally done either by taking the ratio of the emission intensity of two separate lines or using a Boltzmann plot method⁸⁸. In the case of intensity ratios of line emissions, assuming local thermodynamic equilibrium (LTE) in the system, the temperature is estimated using the following equation which is derived from Boltzman equation,

$$\frac{I_1}{I_2} = \frac{g_1 A_1 \lambda_2}{g_2 A_2 \lambda_1} \exp\left(\frac{-(E_1 - E_2)}{k_b T_e}\right) \quad (8)$$

where λ_i , A_i , g_i , I_i and E_i ($i = 1, 2$) are the wavelength, transition probability, statistical weight, line intensity, and energy of the excited state respectively. When only two lines are considered, the selection of these lines is very critical. To have a better accuracy, the upper state energy levels of the two lines under consideration have to be well separated. Moreover, the energy difference should be significantly larger than the plasma electron temperature to get an accurate estimation of electron temperature from line intensity ratio. Also, care has to be taken to make correction for the opacity of the plasma if it is present. A lack of consideration of these conditions can lead to wrong estimation of the temperature. Better estimate of electron temperature can be achieved by using spectral lines of two successive ionization states⁸⁹. Electron temperature can be estimated by eq.2 of this reference.

A more general and accurate way for the estimation of temperature is possible by using the Boltzmann plot method. In this method, a number of lines can be used for the estimation of temperature. The equation for estimating temperature (equation (8)) can be re written as

$$\ln\left[\frac{I_{ij} \lambda_{ij}}{g_i A_{ij}}\right] = \frac{-E_i}{kT_e} + C \quad (9)$$

where I_{ij} , λ_{ij} , A_{ij} , g_i and E_i are the spectral intensity, wavelength, transition probability and statistical weight of the upper state and upper state energy respectively. If a plot is made with E_i on x axis and the left hand

side(LHS) of equation (9) as the y axis, the slope of the graph will be equal to $\frac{-1}{kT_e}$, from which one can easily estimate the plasma temperature. In this method, lines meeting the required conditions can be used, which improves the accuracy of temperature estimation.

Another method for the estimation of plasma temperature using spectroscopy is the line-to-continuum ratio method⁹⁰. The equation for this method is derived from Saha equation and from the expression for the integrated spectral emissivities of the respective lines it can be expressed as

$$\frac{I_1}{\varepsilon_c}(\lambda) = \frac{2.0052 \times 10^{-5} A_{21} g_2 \exp\left(\frac{E_i - \Delta E_1}{kT_e}\right) \exp\left(\frac{-E_2}{kT_e}\right)}{U_i \lambda_i T_e \left[\xi \left(1 - \exp\left(\frac{-hc}{\lambda k T_e}\right)\right) + G \left(\exp\left(\frac{-hc}{\lambda k T_e}\right)\right) \right]} \quad (10)$$

where I_1 is the integrated intensity of emission line, ε_c is the continuum emission coefficient, A_{21} is the transition probability, g_2 is the upper state statistical weight. E_i is the ionization potential, E_2 is the upper state energy level, ΔE_1 is the correction factor to ionization potential due to the plasma which can be neglected safely. U_i is the partition function, ξ is the free-bound continuum correction factor, G is the free free Gaunt factor. Experimentally, ε_c is measured closest to the line chosen. From the above equation we can calculate the electron temperature T_e .

As discussed in case of density, temperature can also be estimated using laser Thomson scattering⁸⁷

IX. LOCAL THERMODYNAMICAL EQUILIBRIUM

For establishing that the levels are populated with Boltzmann distribution, the plasma is assumed to be under local thermodynamic equilibrium (LTE). Macwhirter criterion defined below is taken as a necessary condition for the LTE condition

$$n_e \geq 1.6 \times 10^{12} T_e^{0.5} \Delta E_{mn}^3 \quad (11)$$

where n_e is electron density in cm^{-3} , T_e is electron temperature in Kelvin and ΔE_{mn} (eV) is the largest energy gap between the adjacent energy levels. However for transient and inhomogeneous plasma. Christoferrati criteria⁹¹ discussed below have to be checked. In the case of transient plasma, like the case of a laser produced plasma, require to be verified with the Christoferrati criteria in order to ensure the LTE situation. The Christoferrati criteria state that the diffusion length D_λ of atoms/ions, during a time period of the order of the relaxation time to the equilibrium, should be shorter than the variation length of temperature and electron number density in the plasma. The diffusion length is approximated as

$$D_\lambda \approx 1.4 \times 10^{12} \times \left(\frac{(k_B T_e)^{3/4}}{N_e}\right) \times \left(\frac{\Delta E}{M_A f_{12}(g)}\right)^{1/2} \times e^{\Delta E/2kT_e} \quad (12)$$

where k_B is the Boltzmann constant, N_e is the electron number density, T is the plasma temperature, M_A is the

atomic mass of element, ΔE is the energy difference in the upper and lower level, f_{12} is the oscillator strength and g is the gaunt factor. f_{12} is a dimensionless quantity of the probability of absorption or emission of electromagnetic radiation for a particular transition and g is the correction factor to be used as an approximation to the classical calculation of emission results. Similar to the variations in diffusion length, it is equally important that the relaxation time of the plasma for establishing the thermodynamic equilibrium has to be shorter than the time of variation of plasma temperature and density⁹¹. Typical laser produced plasma at its initial stage has density $\gg 10^{18} cm^{-3}$ and temperature of few eV, which meets the requirement of LTE condition. However, after a sizeable plasma expansion, the density falls rapidly which leads to non-LTE plasma conditions.

X. CALIBRATION FREE LIBS (CFLIBS)

Convention LIBS analysis suffers from matrix effects and also requires reference sample for calibration curve. Hence calibration free LIBS (CF LIBS) approach was adopted. Details of this method are given in a review by Tongoni et al.⁹² and also in recent reference of Zhang et al.³⁵. However, CFLIBS considers that (i) plasma plume represents the actual composition, (ii) the plasma is in LTE condition in spatial as well as temporal window, (iii) plasma is considered to be homogeneous and (iv) the spectral lines under consideration are optically thin.

A. C Sigma graphs

Generalized curves of growth known as CSigma($C\sigma$) graphs which include several lines of various elements of same ionic stage were suggested by Aragon et al. for LIBS⁹³. It is based on Saha, Boltzmann and radiative transfer equations under the assumption of local thermodynamic equilibrium (LTE). Further C-sigma graphs are based on the calculation of line cross section which allows estimation of self-absorption.

B. Internal reference for self-absorption correction (IRSAC)

To overcome self-absorption in CF-LIBS, correction by internal reference has also been suggested⁹⁴. Basically the line chosen as internal reference has lower energy level with higher energy or with low transition probability which is affected slightly by self-absorption. Based on the intensity of other lines can be corrected. Moreover, columnar density and standard reference line (CD-SRL) method has been found to result in better accuracy than standard LIBS^{94,95}.

XI. ENHANCEMENT IN SIGNAL/DETECTION SENSITIVITY

Signal enhancement and subsequent increase in detection sensitivity has been a subject of wide investigations for better exploiting it in various applications. A recent review briefly describes some of the approaches attempted for it². The methods adopted of signal enhancement are DP LIBS, atmosphere control method, applying spatial constraint, application of magnetic and electric fields, microwave assisted LIBS (MALIBS), LIBS/laser induced fluorescence combination (LIBS+LIF), nano particle enhanced LIBS(NELIBS). Sample temperature has also been found to enhance signal emission intensity⁹⁶⁻⁹⁹. Increase in signal emission is attributed to increased ablation rate.

A. Effect of magnetic field

Introduction of magnetic field has been found to result in significant enhancement in the intensity of lines¹⁰⁰. Various mechanisms e.g. confinement by the field, increase in electron impact excitation due to Joule heating and acting as a constraint been suggested for this enhancement^{2,101}.

B. Effect of electric field

Electric field assisted LIBS has been studied for the detection of chlorine and copper¹⁰². In another work significant enhancement (≈ 8 fold) is observed in case of copper lines¹⁰³. Fluctuations (contraction/expansion) in the laser produced plasma are suggested for observed intensity enhancement. Electric field effect on laser induced titanium (Ti) plasma has also been investigated¹⁰⁴. Intensity enhancement in Ti lines has been found to depend on voltage biasing.

C. Glow discharge LIBS (GDLIBS)

GDLIBS has been found to result in significant signal enhancement when compare with simple GD or LIBS¹⁰⁵. GD-LIBS takes advantage of collisional excitation by exciting the material generated by LIBS¹⁰⁶. Flame-enhanced LIBS (FELIBS): Enhancement in LIBS sensitivity was noticed by producing laser plasma in the outer envelope of a neutral oxy-acetylene flame¹⁰⁷. High temperature and low density plasma was observed before $4\mu\text{s}$ which has been projected to be beneficial for enhancing LIBS sensitivity.

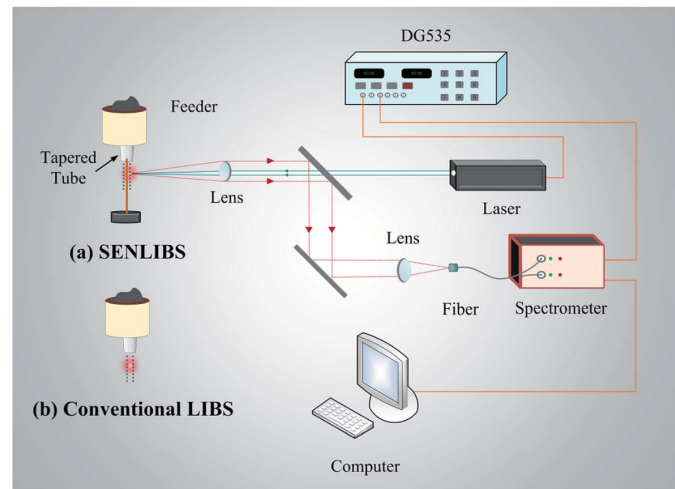


FIG. 14. Schematic diagram of (a) SENLIBS and (b) conventional LIBS (adapted with permission from reference¹¹¹).

D. Microwave Assisted LIBS (MALIBS)

Interaction between microwave radiation and laser produced plasma has been studied in earlier works and significant increase in line intensity was noticed^{108,109}. Intensity enhancement and plasma sustainment in presence of microwave in air has been suggested to occur due to re-excitation and , of course, not due to absorption of the microwave¹¹⁰.

XII. SURFACE ENHANCED LIBS (SENLIBS)

In this method metallic target is used to enhance and stabilise plasma for direct analysis of flow^{111,112}. It has been demonstrated that it has the potential of improving measurement sensitivity. Figure 14 shows the schematic diagram of SENLIBS and conventional LIBS. Figure 15 shows substantial enhancement in the emission intensity for copper and aluminium lines. In both the experiments, it is worth mentioning that there is no significant variation in the background lines.

XIII. LIF+ LIBS

Combination of laser induced fluorescence with LIBS (LIF+LIBS) can enhance the intensity of lines and subsequently provide better detection sensitivity. A typical LIF+LIBS setup is shown in Fig 16, and enhanced Co-I intensity is demonstrated in Fig 17. Significant improvement in single shot Limit of detection is observed while combining LIBS and LIF. Moreover spectral interference effect which is problematic in conventional LIBS can be resolved with LIF +LIBS (adapted with permission from reference¹¹³).

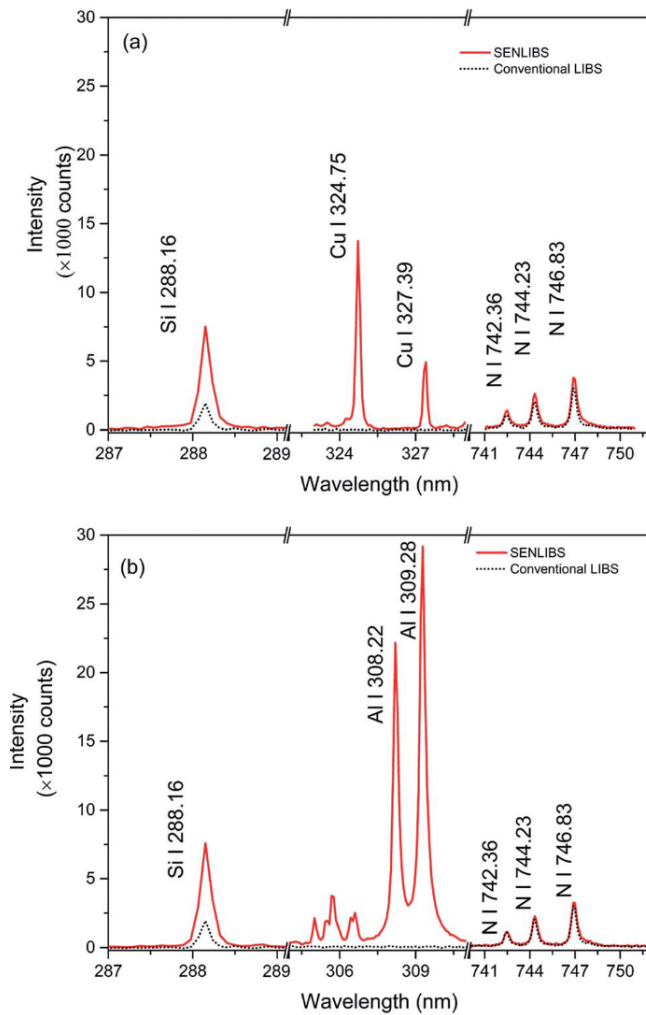


FIG. 15. Spectra showing Si I lines from silica in (a) copper rod and (b) in aluminium rod (adapted with permission from reference¹¹¹).

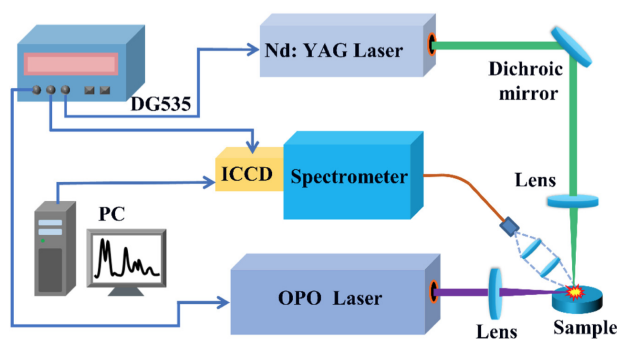


FIG. 16. Typical setup for LIBS+LIF combination (adapted with permission from reference¹¹⁴).

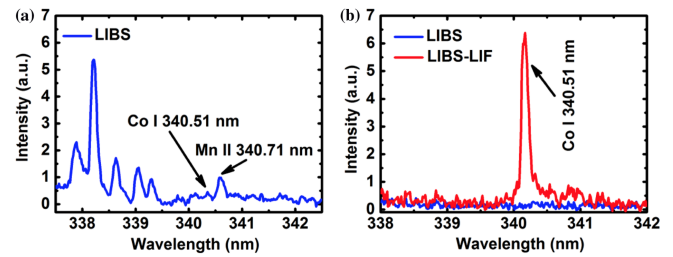


FIG. 17. Enhancement in Co (I) 340.51 nm line in LIBS+LIF (adapted with permission from reference¹¹⁴).

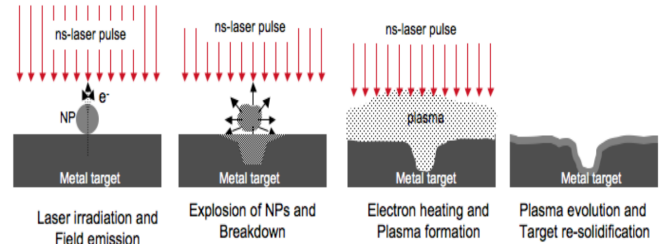


FIG. 18. Schematic of the ablation process in NELIBS: (a) Laser irradiation and field emission, (b) explosion of NPs and breakdown, (c) electron heating and plasma formation, and (d) plasma evolution and target re-solidification (adapted with permission from reference¹¹⁵).

XIV. NANOPARTICLE ENHANCED LIBS (NELIBS)

Presence of nano-particles has been found to enhance LIBS intensity. In Fig 18,19, processes associated in the presence of nano-particle in metallic target are shown. NELIBS has been found to have larger plasma volume and longer persistence in spite of similar plasma parameters. Production of more efficient seed electrons in comparison to conventional LIBS has been attributed to this enhancement.

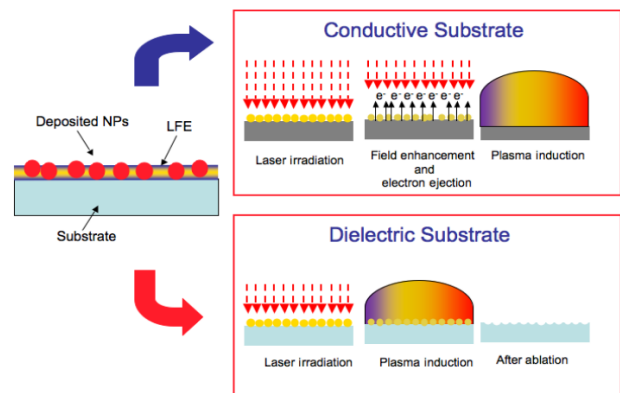


FIG. 19. NP enhanced photo-ablation in metals and dielectrics (adapted with permission from reference²⁶).

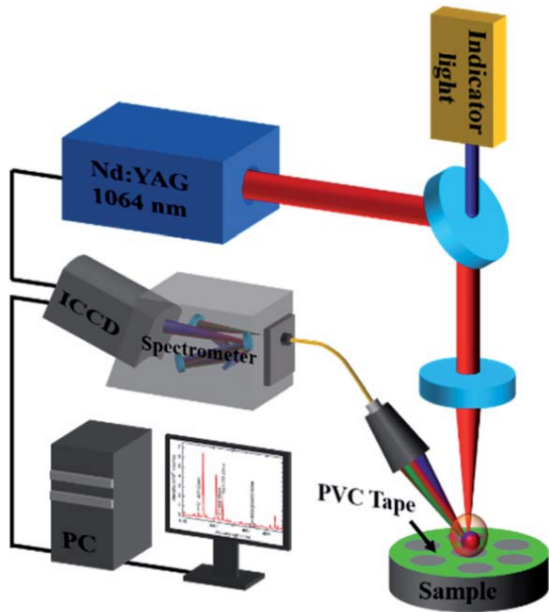


FIG. 20. NEMLIBS set up (adapted with permission from reference¹¹⁶).

Nano-particle enhanced molecular LIBS (NEMLIBS) was recently reported by Tang et.al.¹¹⁶. Geometric constraint was proposed to improve NEMLIBS. Moreover, larger spot size, higher laser energy and pre-ablation of sample are beneficial in NEMLIBS. A typical NEMLIBS set up is shown in figure 20 and enhancement in molecular emission in the absence as well as in the presence of constraint is shown in Fig 21.

XV. SPATIAL CONSTRAINT METHOD

Spatial constraint method: In this method a spatial constraint device is introduced at the periphery of the plasma². The generated shock wave will be reflected at the constraint, subsequently compressing the plasma. This will result in higher temperature and density which in turn will give enhanced signal. A schematic of spatial constraint method is depicted in figure 22.

XVI. OPTICALLY TRAPPED LIBS (OTLIBS)

Optical catapulting-optical trapping LIBS: In this technique spectral identification of micro and nano sized particles is done by sequential optical catapulting, optical trapping and LIBS^{117,118}. The details of optical trapping technique are reviewed in Galbács, et. al²⁵. A typical arrangement for LIBS analysis of optically trapped single particle is illustrated in Fig 23. The method has been demonstrated to have attogram-level detection sensitivity^{117,119}.

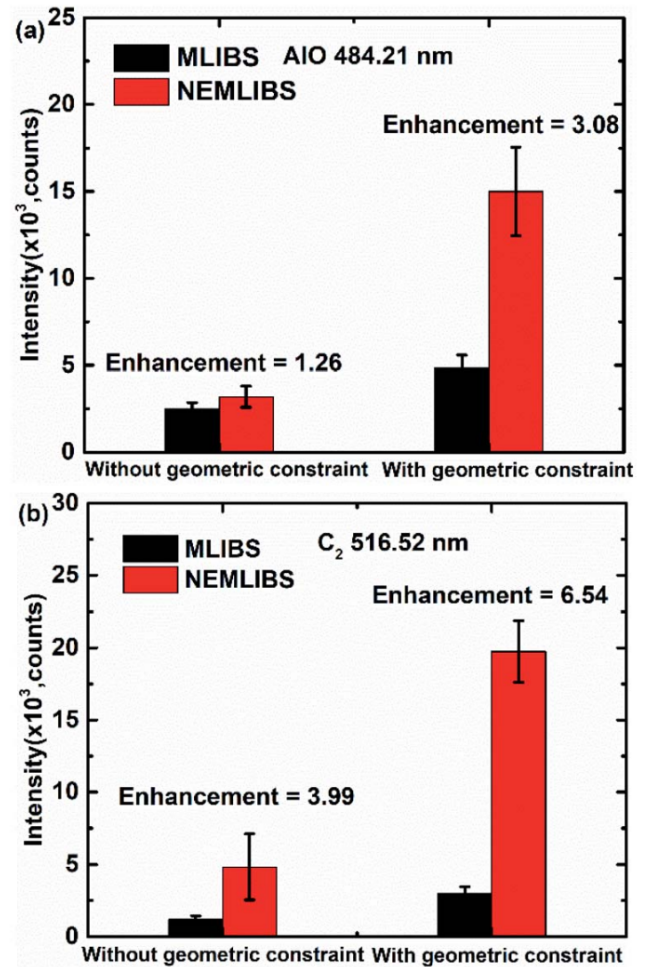


FIG. 21. Demonstration in enhancement in NEMLIBS for AIO and C₂ with and without geometric constraint. (adapted with permission from reference¹¹⁶).

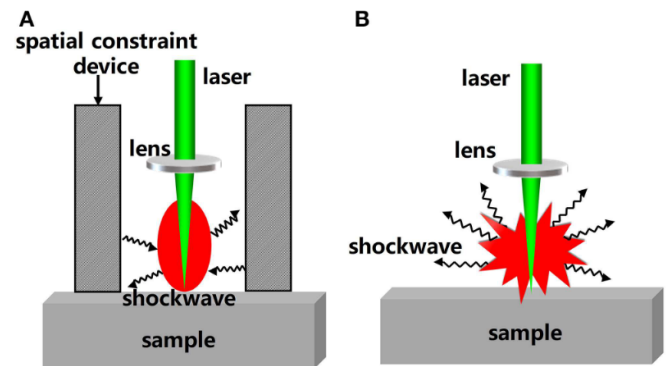


FIG. 22. Plasma plume evolution (A) in the presence of spatial constraint and (B) without spatial constraint (adapted with permission from reference²).

Optically trapped LIBS (OTLIBS)

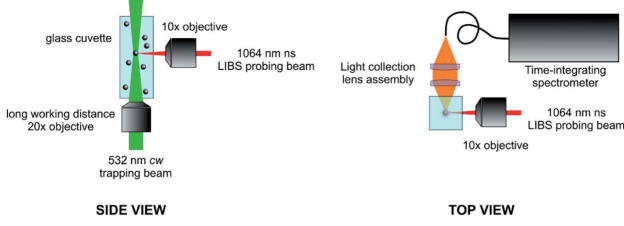


FIG. 23. Scheme of an experimental arrangement for LIBS analysis of optical trapped single nano particles (adapted with permission from reference²⁵).

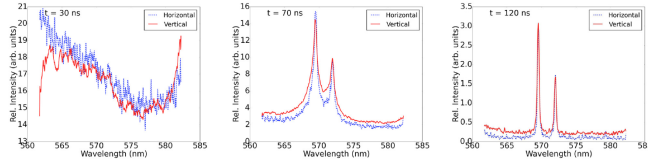


FIG. 24. Polarisation resolved spectra of Al^{2+} for different stages of plasma evolution at a background pressure of 1×10^2 mbar. The laser fluence was $550 J/cm^2$ with an ICCD camera gate width of 10 ns (adapted with permission from reference¹²⁵).

XVII. POLARIZATION RESOLVED LIBS (PRLIBS)

Emission anisotropy in the expanding plasma plume has been studied because of its importance in deciphering electron distribution and self-generated electric and magnetic fields^{120–123}. The degree of polarization at a particular wavelength is defined by

$$P_\lambda = \frac{I_H - I_V}{I_H + I_V} \quad (13)$$

Exploiting polarization resolved LIBS may be interesting in enhancing LIBS sensitivity¹²⁴ as can be seen from figure 24

XVIII. RESONANT ENHANCED LIBS (RELIBS), RESONANT SURFACE ENHANCED LIBS (RSENILIBS)

In RELIBS, the excitation laser is tuned to strong absorption line of one of the major species¹²⁶. The energy absorbed is then distributed over all the elements in the plasma through collisions. A schematic of R-SENILIBS is given in figure 25. Main advantage of RELIBS over LIBS-LIF is its ability to determine multiple species simultaneously. Concept of R-SENILIBS was reported to and was used to detect lead in water¹²⁷. In this method surface enhanced LIBS is combined with resonance enhancement to improve the detection sensitivity. Figure 26 shows the energy level diagram for resonant excitation in the case of Pb atoms. It can be seen that large enhancement in intensity is observed in case of on resonance condition.

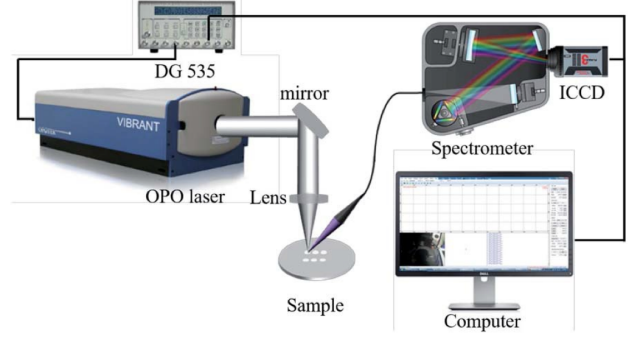


FIG. 25. Schematic of R-SENILIBS set up (adapted with permission from reference¹²⁷).

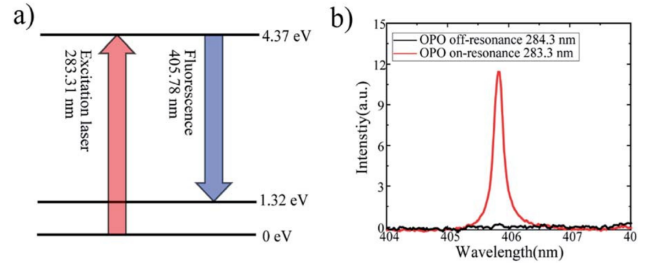


FIG. 26. (a) Partial energy level diagram for resonant excitation of Pb atoms and (b) off resonance and on resonance line spectra (adapted with permission from reference¹²⁷).

XIX. BACK REFLECTION ENHANCED LIBS (BRELIBS)

LIBS sensitivity is enhanced using BRELIBS by using metallic reflectors behind transparent targets¹²⁸ as can be seen in figure 27. In this method metallic reflectors behind target are used to enhance LIBS sensitivity. The reflected laser beam reheats the plasma resulting in enhanced intensity. Further, the obtained LIBS spectrum shows pronounced increase in signal to noise ratio (SNR).

XX. SIMULTANEOUS LIBS COMBINATION WITH OTHER ANALYTICAL MEASUREMENTS

In this section we briefly introduce other analytical methods which are simultaneously used with LIBS.

A. LIBS-Raman

Combination of Raman and LIBS enables one to study the chemical composition in a broader context encompassing elemental and morphological information^{38,39}. In earlier studies simultaneous Raman and LIBS measurements with a single ns laser with 1064 nm fundamental and 532 nm second harmonic were suggested by

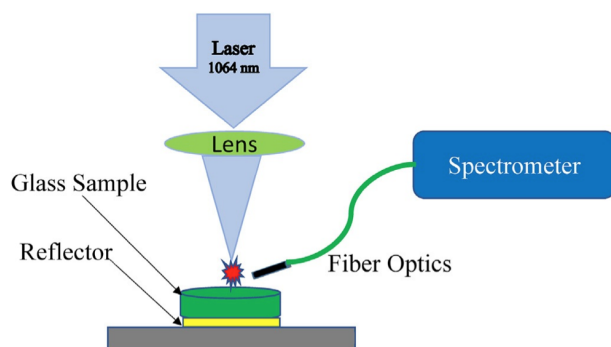


FIG. 27. Schematic of back reflection enhanced LIBS (adapted with permission from reference¹²⁸).

Sharma and coworkers^{129,130}. However, combination of LIBS and Raman in a single platform has gained lot of attention^{131,132}. Spatial and temporal combining techniques have been suggested for this¹³³. Potentially portable table top remote Raman-LIBS system has been reported recently¹³⁴.

B. LIBS-Laser Ablation- Inductively Coupled Plasma (LA-ICP)

Meissner et.al.¹³⁵ compared LIBS and Laser ablation-Inductively coupled mass spectroscopy (LA-ICP-MS) for the detection of trace elements in a solid matrix. LIBS is affected by matrix as well as self-absorption but does not depend on sample preparation. On the other hand, LA-ICP-MS detection limits are in principle lower but the preparation method strongly influences the measurements. Simultaneous LIBS and LA-ICP optical emission spectroscopy (LA-ICP-OES) have been reported for simultaneous analysis of the elements in asphaltene¹³⁶. Elemental analysis was done by LA-ICP-MS as well. At the same time the aromatic/paraffinic nature was also determined by LIBS from H/C ratio. Simultaneous LIBS and LA-ICP- mass spectroscopy (LA-ICP-MS) has been reported for spatially resolved mapping of major and trace elements Bastnasite rare earth ore¹³⁷. The combination of two techniques provides complementary measurements that can be achieved with separate measurements due to low sensitivity or strong interferences. Combined LIBS/LA-ICP-MS has been reported for polymer alteration under corrosive conditions¹³⁸. It has been demonstrated that LIBS/LA-ICP-MS is a powerful method for polymer characterization as well in the study of polymer degradation.

C. LIBS- X-Ray Fluorescence (XRF)

Double pulse LIBS and micro-x-ray fluorescence (micro-XRF) were reported for characterizing materials¹³⁹. They have found that LIBS is highly subjective to sample chemical and physical properties. Performance of portable LIBS and portable XRF device has been reported by Rao et. al¹⁴⁰. While portable LIBS can give instantaneous measurement, its accuracy is hampered by self-absorption. On the other hand, XRF measurements have better limit of detection but the measurement consumes time.

XXI. CONCLUDING REMARKS

In this brief review we sketch LIBS techniques from parameter estimation to the emerging trends and also projected applications. In this article we have also introduced application aspects of some hitherto not exploited much phenomena e.g. colliding plasma, self-reversal of lines and GIBS. Further, we believe that glimpses outlined in the present review will provide a sound platform to the beginners also as it encompasses brief phenomenological aspects as well as recent developments in the field.

XXII. REFERENCES

- ¹K. Berlo, W. Xia, F. Zwillich, E. Gibbons, R. Gaudiuso, E. Ewusi-Annan, G. R. Chiklis, and N. Melikechi, "Laser induced breakdown spectroscopy for the rapid detection of sars-cov-2 immune response in plasma," *Scientific Reports* **12**, 1614 (2022).
- ²X. Fu, G. Li, and D. Dong, "Improving the detection sensitivity for laser-induced breakdown spectroscopy: A review," *Frontiers in Physics* **8**, 68 (2020).
- ³D. F. Andrade, E. R. Pereira-Filho, and D. Amarasiriwardena, "Current trends in laser-induced breakdown spectroscopy: a tutorial review," *Applied Spectroscopy Reviews* **56**, 98–114 (2021), <https://doi.org/10.1080/05704928.2020.1739063>.
- ⁴G. S. Senesi, R. S. Harmon, and R. R. Hark, "Field-portable and handheld laser-induced breakdown spectroscopy: Historical review, current status and future prospects," *Spectrochimica Acta Part B: Atomic Spectroscopy* **175**, 106013 (2021).
- ⁵E. Mal, R. Junjuri, M. K. Gundawar, and A. Khare, "Optimization of temporal window for application of calibration free-laser induced breakdown spectroscopy (cf-libS) on copper alloys in air employing a single line," *J. Anal. At. Spectrom.* **34**, 319–330 (2019).
- ⁶G. Arora, J. Thomas, and H. C. Joshi, "On the delayed emission from a laser-produced aluminum plasma under an argon environment," *J. Anal. At. Spectrom.* **37**, 1119–1125 (2022).
- ⁷D. W. Hahn and N. Omenetto, "Laser-induced breakdown spectroscopy (libs), part ii: Review of instrumental and methodological approaches to material analysis and applications to different fields," *Appl. Spectrosc.* **66**, 347–419 (2012).
- ⁸D. W. Hahn and N. Omenetto, "Laser-induced breakdown spectroscopy (libs), part i: Review of basic diagnostics and plasma-particle interactions: Still-challenging issues within the analytical plasma community," *Appl. Spectrosc.* **64**, 335A–366A (2010).

- ⁹C. Pasquini, J. Cortez, L. Silva, and F. B. Gonzaga, "Laser induced breakdown spectroscopy," *Journal of the Brazilian Chemical Society* **18**, 463–512 (2007).
- ¹⁰J. P. Singh and S. N. Thakur, *Laser-induced breakdown spectroscopy* (Elsevier, 2020).
- ¹¹J. P. Singh and S. N. Thakur, *Laser-Induced Breakdown Spectroscopy* (Elsevier, 2007).
- ¹²A. W. Miziolek, V. Palleschi, and I. Schechter, *Laser induced breakdown spectroscopy* (Cambridge university press, 2006).
- ¹³A. F. Pablo, *A Guide to Laser-induced Breakdown Spectroscopy* (Nova Science Pub Inc, 2021).
- ¹⁴R. Noll, "Laser-induced breakdown spectroscopy," in *Laser-Induced Breakdown Spectroscopy* (Springer, 2012) pp. 7–15.
- ¹⁵D. Zhang, H. Zhang, Y. Zhao, Y. Chen, C. Ke, T. Xu, and Y. He, "A brief review of new data analysis methods of laser-induced breakdown spectroscopy: machine learning," *Applied Spectroscopy Reviews* **57**, 89–111 (2022), <https://doi.org/10.1080/05704928.2020.1843175>.
- ¹⁶S. Romppanen, I. Pölonen, H. Häkkänen, and S. Kaski, "Optimization of spodumene identification by statistical approach for laser-induced breakdown spectroscopy data of lithium pegmatite ores," *Applied Spectroscopy Reviews* **0**, 1–21 (2021), <https://doi.org/10.1080/05704928.2021.1963977>.
- ¹⁷O. A. Al-Najjar, Y. S. Wudil, U. F. Ahmad, O. S. B. Al-Amoudi, M. A. Al-Osta, and M. A. Gondal, "Applications of laser induced breakdown spectroscopy in geotechnical engineering: a critical review of recent developments, perspectives and challenges," *Applied Spectroscopy Reviews* **0**, 1–37 (2022), <https://doi.org/10.1080/05704928.2022.2136192>.
- ¹⁸D. F. Andrade, E. R. Pereira-Filho, and D. Amarasiriwardena, "Current trends in laser-induced breakdown spectroscopy: a tutorial review," *Applied Spectroscopy Reviews* **56**, 98–114 (2021), <https://doi.org/10.1080/05704928.2020.1739063>.
- ¹⁹E. J. Kautz, E. N. Weerakkody, M. S. Finko, D. Curreli, B. Koroglu, T. P. Rose, D. G. Weisz, J. C. Crowhurst, H. B. Radousky, M. DeMagistris, N. Sinha, D. A. Levin, E. L. Dreizin, M. C. Phillips, N. G. Glumac, and S. S. Harilal, "Optical spectroscopy and modeling of uranium gas-phase oxidation: Progress and perspectives," *Spectrochimica Acta Part B: Atomic Spectroscopy* **185**, 106283 (2021).
- ²⁰G. S. Maurya, A. Marín-Roldán, P. Veis, A. K. Pathak, and P. Sen, "A review of the libs analysis for the plasma-facing components diagnostics," *Journal of Nuclear Materials* **541**, 152417 (2020).
- ²¹C. Li, C.-L. Feng, H. Y. Oderji, G.-N. Luo, and H.-B. Ding, "Review of libs application in nuclear fusion technology," *Frontiers of Physics* **11**, 1–16 (2016).
- ²²L. Jolivet, M. Leprince, S. Moncayo, L. Sorbier, C.-P. Liemann, and V. Motto-Ros, "Review of the recent advances and applications of libs-based imaging," *Spectrochimica Acta Part B: Atomic Spectroscopy* **151**, 41–53 (2019).
- ²³J. D. Pedarnig, S. Trautner, S. Grünberger, N. Giannakaris, S. Eschlböck-Fuchs, and J. Hofstadler, "Review of element analysis of industrial materials by in-line laser-induced breakdown spectroscopy (libs)," (2021).
- ²⁴D. Zhang, H. Zhang, Y. Zhao, Y. Chen, C. Ke, T. Xu, and Y. He, "A brief review of new data analysis methods of laser-induced breakdown spectroscopy: machine learning," *Applied Spectroscopy Reviews* **0**, 1–23 (2020), <https://doi.org/10.1080/05704928.2020.1843175>.
- ²⁵G. Galbács, A. Kéri, A. Kohut, M. Veres, and Z. Geretovszky, "Nanoparticles in analytical laser and plasma spectroscopy – a review of recent developments in methodology and applications," *J. Anal. At. Spectrom.* **36**, 1826–1872 (2021).
- ²⁶M. Dell’Aglia, R. Alrfai, and A. De Giacomo, "Nanoparticle enhanced laser induced breakdown spectroscopy (nelibs), a first review," *Spectrochimica Acta Part B: Atomic Spectroscopy* **148**, 105–112 (2018).
- ²⁷S. Legnaioli, B. Campanella, F. Poggialini, S. Pagnotta, M. A. Harith, Z. A. Abdel-Salam, and V. Palleschi, "Industrial applications of laser-induced breakdown spectroscopy: a review," *Anal. Methods* **12**, 1014–1029 (2020).
- ²⁸A. MATSUMOTO and T. SAKKA, "A review of underwater laser-induced breakdown spectroscopy of submerged solids," *Analytical Sciences* **37**, 1061–1072 (2021).
- ²⁹D. Stefan, N. Gyftokostas, E. Nanou, P. Kourelis, and S. Couris, "Laser-induced breakdown spectroscopy: An efficient tool for food science and technology (from the analysis of martian rocks to the analysis of olive oil, honey, milk, and other natural earth products)," *Molecules* **26** (2021), [10.3390/molecules26164981](https://doi.org/10.3390/molecules26164981).
- ³⁰E. J. Kautz, A. Devaraj, D. J. Senor, and S. S. Harilal, "Hydrogen isotopic analysis of nuclear reactor materials using ultrafast laser-induced breakdown spectroscopy," *Opt. Express* **29**, 4936–4946 (2021).
- ³¹M. Burger, P. J. Skrodzki, I. Jovanovic, M. C. Phillips, and S. S. Harilal, "Laser-produced uranium plasma characterization and stark broadening measurements," *Physics of Plasmas* **26**, 093103 (2019), <https://doi.org/10.1063/1.5099643>.
- ³²M. N. Khan, Q. Wang, B. S. Idrees, W. Xiangli, G. Teng, X. Cui, Z. Zhao, K. Wei, and M. Abrar, "A review on laser-induced breakdown spectroscopy in different cancers diagnosis and classification," *Frontiers in Physics* **10** (2022), [10.3389/fphy.2022.821057](https://doi.org/10.3389/fphy.2022.821057).
- ³³H. Ji, Y. Ding, L. Zhang, Y. Hu, and X. Zhong, "Review of aerosol analysis by laser-induced breakdown spectroscopy," *Applied Spectroscopy Reviews* **56**, 193–220 (2021), <https://doi.org/10.1080/05704928.2020.1780604>.
- ³⁴S. Qiao, Y. Ding, D. Tian, L. Yao, and G. Yang, "A review of laser-induced breakdown spectroscopy for analysis of geological materials," *Applied Spectroscopy Reviews* **50**, 1–26 (2015), <https://doi.org/10.1080/05704928.2014.911746>.
- ³⁵N. Zhang, T. Ou, M. Wang, Z. Lin, C. Lv, Y. Qin, J. Li, H. Yang, N. Zhao, and Q. Zhang, "A brief review of calibration-free laser-induced breakdown spectroscopy," *Frontiers in Physics* **10** (2022), [10.3389/fphy.2022.887171](https://doi.org/10.3389/fphy.2022.887171).
- ³⁶N.-H. Cheung, "Laser-induced plume fluorescence for ultra-sensitive and simultaneous multianalyte analysis – a review," *Spectrochimica Acta Part B: Atomic Spectroscopy* **194**, 106473 (2022).
- ³⁷M. C. S. Ribeiro, G. S. Senesi, J. S. Cabral, C. Cena, B. S. Marangoni, C. Kiefer, and G. Nicolodelli, "Evaluation of rice varieties using libs and ftir techniques associated with pca and machine learning algorithms," *Appl. Opt.* **59**, 10043–10048 (2020).
- ³⁸D. Holub, P. Porizka, M. Kizovsky, D. Prochazka, O. Samek, and J. Kaiser, "The potential of combining laser-induced breakdown spectroscopy and raman spectroscopy data for the analysis of wood samples," *Spectrochimica Acta Part B: Atomic Spectroscopy* **195**, 106487 (2022).
- ³⁹H. Sun, C. Song, X. Lin, and X. Gao, "Identification of meat species by combined laser-induced breakdown and raman spectroscopies," *Spectrochimica Acta Part B: Atomic Spectroscopy* **194**, 106456 (2022).
- ⁴⁰C. Sandoval-Munoz, G. Velasquez, J. Alvarez, F. Perez, M. Velasquez, S. Torres, D. Sbarbaro-Hofer, V. Motto-Ros, and J. Yanez, "Enhanced elemental and mineralogical imaging of cu-mineralized rocks by coupling ?-libs and hsi," *J. Anal. At. Spectrom.* **37**, 1981–1993 (2022).
- ⁴¹D. V. S, S. D. George, V. B. Kartha, S. Chidangil, and U. V. K, "Hybrid libs-raman-lif systems for multi-modal spectroscopic applications: a topical review," *Applied Spectroscopy Reviews* **56**, 463–491 (2021), <https://doi.org/10.1080/05704928.2020.1800486>.
- ⁴²H. van der Meiden, S. Almaviva, J. Butikova, V. Dwivedi, P. Gasior, W. Gromelski, A. Hakola, X. Jiang, I. Jögi, J. Karhunen, M. Kubkowska, M. Laan, G. Maddaluno, A. Marín-Roldán, P. Paris, K. Piip, M. Pisarcik, G. Sergienko,

- M. Veis, P. Veis, S. Brezinsek, and the EUROfusion WP PFC Team, "Monitoring of tritium and impurities in the first wall of fusion devices using a LIBS based diagnostic," *Nuclear Fusion* **61**, 125001 (2021).
- ⁴³N. L. LaHaye, S. S. Harilal, P. K. Diwakar, and A. Hassanein, "The effect of laser pulse duration on icp-ms signal intensity, elemental fractionation, and detection limits in fs-la-icp-ms," *J. Anal. At. Spectrom.* **28**, 1781–1787 (2013).
- ⁴⁴S. S. Harilal, B. E. Brumfield, B. D. Cannon, and M. C. Phillips, "Shock wave mediated plume chemistry for molecular formation in laser ablation plasmas," *Analytical Chemistry* **88**, 2296–2302 (2016), pMID: 26732866, <https://doi.org/10.1021/acs.analchem.5b04136>.
- ⁴⁵J. Thomas, H. C. Joshi, A. Kumar, and R. Philip, "Pulse width dependent dynamics of laser-induced plasma from a ni thin film," *Journal of Physics D: Applied Physics* **52**, 135201 (2019).
- ⁴⁶K. K. Anoop, S. S. Harilal, R. Philip, R. Bruzzese, and S. Amoroso, "Laser fluence dependence on emission dynamics of ultrafast laser induced copper plasma," *Journal of Applied Physics* **120**, 185901 (2016), <https://doi.org/10.1063/1.4967313>.
- ⁴⁷N. Smijesh and R. Philip, "Emission dynamics of an expanding ultrafast-laser produced zn plasma under different ambient pressures," *Journal of Applied Physics* **114**, 093301 (2013), <https://doi.org/10.1063/1.4820575>.
- ⁴⁸A. Mondal, R. K. Singh, and A. Kumar, "Effect of ablation geometry on the dynamics, composition, and geometrical shape of thin film plasma," *Physics of Plasmas* **25**, 013517 (2018), <https://doi.org/10.1063/1.4991469>.
- ⁴⁹L. Escobar-Alarcón, E. Camps, E. Haro-Poniatowski, M. Villagran, and C. Sanchez, "Characterization of rear- and front-side laser ablation plasmas for thin-film deposition," *Applied Surface Science* **197–198**, 192–196 (2002).
- ⁵⁰A. Mondal, R. K. Singh, and H. C. Joshi, "Neutral and ion composition of laser produced lithium plasma plume in front and back ablation of thin film," *J. Anal. At. Spectrom.* **34**, 1822–1828 (2019).
- ⁵¹E. Képeš, I. Gornushkin, P. Pořízka, and J. Kaiser, "Spatiotemporal spectroscopic characterization of plasmas induced by non-orthogonal laser ablation," *Analyst* **146**, 920–929 (2021).
- ⁵²N. Li, N. Nishi, R. Zheng, and T. Sakka, "Signal enhancement in underwater long-pulse laser-induced breakdown spectroscopy for the analysis of bulk water," *J. Anal. At. Spectrom.* **36**, 1170–1179 (2021).
- ⁵³N. Li, K. Tanabe, N. Nishi, R. Zheng, and T. Sakka, "Simultaneous detection of a submerged cu target and bulk water by long-pulse laser-induced breakdown spectroscopy," *J. Anal. At. Spectrom.* **36**, 1960–1968 (2021).
- ⁵⁴P. Diwakar, S. Harilal, J. Freeman, and A. Hassanein, "Role of laser pre-pulse wavelength and inter-pulse delay on signal enhancement in collinear double-pulse laser-induced breakdown spectroscopy," *Spectrochimica Acta Part B: Atomic Spectroscopy* **87**, 65–73 (2013), thematic Issue: 7th International Conference on Laser Induced Breakdown Spectroscopy (LIBS 2012), Luxor, Egypt, 29 September–4 October 2012.
- ⁵⁵Y. Wang, A. Chen, D. Zhang, Q. Wang, S. Li, Y. Jiang, and M. Jin, "Enhanced optical emission in laser-induced breakdown spectroscopy by combining femtosecond and nanosecond laser pulses," *Physics of Plasmas* **27**, 023507 (2020), <https://doi.org/10.1063/1.5131772>.
- ⁵⁶N. Giannakaris, A. Haider, C. M. Ahamer, S. Grünberger, S. Trautner, and J. D. Pedarnig, "Femtosecond single-pulse and orthogonal double-pulse laser-induced breakdown spectroscopy (libs): Femtogram mass detection and chemical imaging with micrometer spatial resolution," *Applied Spectroscopy* **0**, 00037028211042398 (0), pMID: 34494912, <https://doi.org/10.1177/00037028211042398>.
- ⁵⁷Y. Sivakumaran, H. C. Joshi, R. K. Singh, and A. Kumar, "Optical time of flight studies of lithium plasma in double pulse laser ablation: Evidence of inverse bremsstrahlung absorption," *Physics of Plasmas* **21**, 063110 (2014), <https://doi.org/10.1063/1.4885107>.
- ⁵⁸J. Wang, Y. Zhao, G. Wang, L. Zhang, S. Wang, W. Zhang, X. Ma, Z. Liu, X. Luo, W. Ma, Z. Ye, Z. Zhu, W. Yin, and S. Jia, "Theoretical study on signal enhancement of orthogonal double pulse induced plasma," *J. Anal. At. Spectrom.* , – (2022).
- ⁵⁹P. Hough, C. McLoughlin, S. S. Harilal, J. P. Mosnier, and J. T. Costello, "Emission characteristics and dynamics of the stagnation layer in colliding laser produced plasmas," *Journal of Applied Physics* **107**, 024904 (2010), <https://doi.org/10.1063/1.3282683>.
- ⁶⁰K. F. Al-Shboul, S. S. Harilal, S. M. Hassan, A. Hassanein, J. T. Costello, T. Yabuuchi, K. A. Tanaka, and Y. Hirooka, "Interpenetration and stagnation in colliding laser plasmas," *Physics of Plasmas* **21**, 013502 (2014), <https://doi.org/10.1063/1.4859136>.
- ⁶¹A. K. Saxena, R. K. Singh, H. C. Joshi, and A. Kumar, "Spectroscopic investigation of molecular formation in laterally colliding laser-produced carbon plasmas," *Appl. Opt.* **58**, 561–570 (2019).
- ⁶²A. Mondal, R. K. Singh, V. Chaudhari, and H. C. Joshi, "Effect of magnetic field on the lateral interaction of plasma plumes," *Physics of Plasmas* **27**, 093109 (2020), <https://doi.org/10.1063/5.0006647>.
- ⁶³P. K. Tiwari, N. Behera, R. Singh, and H. Joshi, "Comparative study of libs signal for single and colliding plasma plumes in a variable magnetic field," *Spectrochimica Acta Part B: Atomic Spectroscopy* **191**, 106411 (2022).
- ⁶⁴B. Delaney, P. Hayden, T. Kelly, E. Kennedy, and J. Costello, "Laser induced breakdown spectroscopy with annular plasmas in vacuo: Stagnation and limits of detection," *Spectrochimica Acta Part B: Atomic Spectroscopy* **193**, 106430 (2022).
- ⁶⁵P. Rohwetter, K. Stelmaszczyk, L. Wöste, R. Ackermann, G. Méjean, E. Salmon, J. Kasparian, J. Yu, and J.-P. Wolf, "Filament-induced remote surface ablation for long range laser-induced breakdown spectroscopy operation," *Spectrochimica Acta Part B: Atomic Spectroscopy* **60**, 1025–1033 (2005), laser Induced Plasma Spectroscopy and Applications (LIBS 2004) Third International Conference.
- ⁶⁶V. Motto-Ros, S. Moncayo, C. Fabre, and B. Busser, "Chapter 14 - libs imaging applications," in *Laser-Induced Breakdown Spectroscopy (Second Edition)*, edited by J. P. Singh and S. N. Thakur (Elsevier, Amsterdam, 2020) second edition ed., pp. 329–346.
- ⁶⁷M. Hu, J. Peng, S. Niu, and H. Zeng, "Plasma-grating-induced breakdown spectroscopy," *Advanced Photonics* **2**, 1 – 6 (2020).
- ⁶⁸W. Huang, C. He, Y. Wang, W. Zhao, and L. Qiu, "Confocal controlled libs microscopy with high spatial resolution and stability," *J. Anal. At. Spectrom.* **35**, 2530–2535 (2020).
- ⁶⁹F. Rezaei, G. Cristoforetti, E. Tognoni, S. Legnaioli, V. Palleschi, and A. Safi, "A review of the current analytical approaches for evaluating, compensating and exploiting self-absorption in laser induced breakdown spectroscopy," *Spectrochimica Acta Part B: Atomic Spectroscopy* **169**, 105878 (2020).
- ⁷⁰Y. Yang, X. Hao, and L. Ren, "Correction of self-absorption effect in calibration-free laser-induced breakdown spectroscopy(cf-libs) by considering plasma temperature and electron density," *Optik* **208**, 163702 (2020).
- ⁷¹K. Touchet, F. Chartier, J. Hermann, and J.-B. Sirven, "Laser-induced breakdown self-reversal isotopic spectrometry for isotopic analysis of lithium," *Spectrochimica Acta Part B: Atomic Spectroscopy* **168**, 105868 (2020).
- ⁷²B. Kumar, R. K. Singh, and A. Kumar, "Dynamics of laser-blow-off induced li plume in confined geometry," *Physics of Plasmas* **20**, 083511 (2013), <https://doi.org/10.1063/1.4818900>.
- ⁷³M. Kumar, N. Behera, R. Singh, and H. Joshi, "Optical time-of-flight and spectroscopic investigation of laser produced barium plasma in presence of magnetic field and ambient gas," *Physics Letters A* **429**, 127968 (2022).

- ⁷⁴I. Urbina, F. Bredice, C. Sanchez-Aké, M. Villagrán-Muniz, and V. Palleschi, "Temporal analysis of self-reversed σ resonant lines in libs experiment at different laser pulse energy and in different surrounding media," *Spectrochimica Acta Part B: Atomic Spectroscopy* **195**, 106489 (2022).
- ⁷⁵E. J. Kautz, M. C. Phillips, and S. S. Harilal, "Laser-induced fluorescence of filament-produced plasmas," *Journal of Applied Physics* **130**, 203302 (2021), <https://doi.org/10.1063/5.0065240>.
- ⁷⁶R. Mayo, M. Ortiz, and M. Plaza, "Measured stark widths of several ni II spectral lines," *Journal of Physics B: Atomic, Molecular and Optical Physics* **41**, 095702 (2008).
- ⁷⁷C. Aragon, J. Aguilera, and J. Manrique, "Measurement of stark broadening parameters of fe ii and ni ii spectral lines by laser induced breakdown spectroscopy using fused glass samples," *Journal of Quantitative Spectroscopy and Radiative Transfer* **134**, 39–45 (2014).
- ⁷⁸J. Manrique, J. A. Aguilera, and C. Aragon, "Experimental Stark widths and shifts of Ti ii spectral lines," *Monthly Notices of the Royal Astronomical Society* **462**, 1501–1507 (2016), <https://academic.oup.com/mnras/article-pdf/462/2/1501/13773749/stw1641.pdf>.
- ⁷⁹J. Thomas, H. C. Joshi, A. Kumar, and R. Philip, "Effect of ambient gas pressure on nanosecond laser produced plasma on nickel thin film in a forward ablation geometry," *Physics of Plasmas* **25**, 103108 (2018), <https://doi.org/10.1063/1.5048834>.
- ⁸⁰A. El Sherbini, H. Hegazy, and T. El Sherbini, "Measurement of electron density utilizing the h-alpha line from laser produced plasma in air," *Spectrochimica Acta Part B: Atomic Spectroscopy* **61**, 532–539 (2006).
- ⁸¹D. Nishijima and R. P. Doerner, "Stark width measurements and boltzmann plots of w i in nanosecond laser-induced plasmas," *Journal of Physics D: Applied Physics* **48**, 325201 (2015).
- ⁸²H. Liu, B. S. Truscott, and M. N. R. Ashfold, "Determination of stark parameters by cross-calibration in a multi-element laser-induced plasma," *Scientific Reports* **6**, 25609 (2016).
- ⁸³F. Poggialini, B. Campanella, R. Jafer, S. Legnaioli, F. Bredice, S. Raneri, and V. Palleschi, "Determination of the stark broadening coefficients of tantalum emission lines by time-independent extended c-sigma method," *Spectrochimica Acta Part B: Atomic Spectroscopy* **167**, 105829 (2020).
- ⁸⁴H. Griem, *Spectral Line Broadening by Plasmas* (Academic Press, New York, 1974).
- ⁸⁵S. S. Harilal, M. C. Phillips, D. H. Froula, K. K. Anoop, R. C. Issac, and F. N. Beg, "Optical diagnostics of laser-produced plasmas," *Rev. Mod. Phys.* **94**, 035002 (2022).
- ⁸⁶K. Choudhury, R. K. Singh, S. Narayan, A. Srivastava, and A. Kumar, "Time resolved interferometric study of the plasma plume induced shock wave in confined geometry: Two-dimensional mapping of the ambient and plasma density," *Physics of Plasmas* **23**, 042108 (2016), <https://doi.org/10.1063/1.4947032>.
- ⁸⁷K. Muraoka and A. Kono, "Laser thomson scattering for low-temperature plasmas," *Journal of Physics D: Applied Physics* **44**, 043001 (2011).
- ⁸⁸C. Aragon and J. Aguilera, "Characterization of laser induced plasmas by optical emission spectroscopy: A review of experiments and methods," *Spectrochimica Acta Part B: Atomic Spectroscopy* **63**, 893 – 916 (2008).
- ⁸⁹S. S. Harilal, C. V. Bindhu, V. P. N. Nampoore, and C. P. G. Vallabhan, "Time evolution of the electron density and temperature in laser-produced plasmas from yba2cu3o7," *Applied Physics B* **66**, 633–638 (1998).
- ⁹⁰H.-Y. Moon, B. W. Smith, and N. Omenetto, "Temporal behavior of line-to-continuum ratios and ion fractions as a means of assessing thermodynamic equilibrium in laser-induced breakdown spectroscopy," *Chemical Physics* **398**, 221 – 227 (2012), *chemical Physics of Low-Temperature Plasmas (in honour of Prof Mario Capitelli)*.
- ⁹¹G. Cristoforetti, A. D. Giacomo, M. Dell'Aglio, S. Legnaioli, E. Tognoni, V. Palleschi, and N. Omenetto, "Local thermodynamic equilibrium in laser-induced breakdown spectroscopy: Beyond the mcwhirter criterion," *Spectrochimica Acta Part B: Atomic Spectroscopy* **65**, 86 – 95 (2010).
- ⁹²E. Tognoni, G. Cristoforetti, S. Legnaioli, and V. Palleschi, "Calibration-free laser-induced breakdown spectroscopy: State of the art," *Spectrochimica Acta Part B: Atomic Spectroscopy* **65**, 1–14 (2010).
- ⁹³C. Aragon and J. Aguilera, "Csigma graphs: A new approach for plasma characterization in laser-induced breakdown spectroscopy," *Journal of Quantitative Spectroscopy and Radiative Transfer* **149**, 90–102 (2014).
- ⁹⁴L. Sun and H. Yu, "Correction of self-absorption effect in calibration-free laser-induced breakdown spectroscopy by an internal reference method," *Talanta* **79** **2**, 388–95 (2009).
- ⁹⁵Z. Hu, F. Chen, D. Zhang, Y. Chu, W. Wang, Y. Tang, and L. Guo, "A method for improving the accuracy of calibration-free laser-induced breakdown spectroscopy by exploiting self-absorption," *Analytica Chimica Acta* **1183**, 339008 (2021).
- ⁹⁶R. Hai, Z. He, D. Wu, W. Tong, H. Sattar, M. Imran, and H. Ding, "Influence of sample temperature on the laser-induced breakdown spectroscopy of a molybdenum-tungsten alloy," *J. Anal. At. Spectrom.* **34**, 2378–2384 (2019).
- ⁹⁷V. N. Lednev, M. Y. Grishin, P. A. Sdvizhenskii, R. D. Asyutin, R. S. Tretyakov, A. Y. Stavertiy, and S. M. Pershin, "Sample temperature effect on laser ablation and analytical capabilities of laser induced breakdown spectroscopy," *J. Anal. At. Spectrom.* **34**, 607–615 (2019).
- ⁹⁸K. Guo, A. Chen, W. Xu, D. Zhang, and M. Jin, "Effect of sample temperature on time-resolved laser-induced breakdown spectroscopy," *AIP Advances* **9**, 065214 (2019), <https://doi.org/10.1063/1.5097301>.
- ⁹⁹S. Tavassoli and A. Gragossian, "Effect of sample temperature on laser-induced breakdown spectroscopy," *Optics & Laser Technology* **41**, 481–485 (2009).
- ¹⁰⁰V. N. Rai, H. Zhang, F. Y. Yueh, J. P. Singh, and A. Kumar, "Effect of steady magnetic field on laser-induced breakdown spectroscopy," *Appl. Opt.* **42**, 3662–3669 (2003).
- ¹⁰¹H. Joshi, A. Kumar, R. Singh, and V. Prahlad, "Effect of a transverse magnetic field on the plume emission in laser-produced plasma: An atomic analysis," *Spectrochimica Acta Part B: Atomic Spectroscopy* **65**, 415–419 (2010).
- ¹⁰²R. Ahmed, A. Jabbar, M. Akhtar, Z. A. Umar, and M. A. Baig, "Amelioration in the detection of chlorine using electric field assisted libs," *Plasma Chemistry and Plasma Processing* **40**, 809–818 (2020).
- ¹⁰³R. AHMED, A. JABBAR, Z. A. UMAR, and M. A. BAIG, "Electric-field induced fluctuations in laser generated plasma plume," *Plasma Science and Technology* **23**, 045505 (2021).
- ¹⁰⁴E. Asamoah, C. Jiawei, K. Ayepah, S. Wilson, Y. Hongbing, Z. Weihua, Z. Lin, W. Pengyu, and A. Asamoah, "Investigating a laser-induced titanium plasma under an applied static electric field," *Spectroscopy (Santa Monica)* **36** (2021), cited By 1.
- ¹⁰⁵K. A. Terezchuk, J. M. Vadillo, and J. J. Laserna, "Glow-discharge-assisted laser-induced breakdown spectroscopy: Increased sensitivity in solid analysis," *Appl. Spectrosc.* **62**, 1262–1267 (2008).
- ¹⁰⁶K. Terezchuk, J. Vadillo, and J. Laserna, "Depth profile analysis of layered samples using glow discharge assisted laser-induced breakdown spectrometry (gd-libs)," *Spectrochimica Acta Part B: Atomic Spectroscopy* **64**, 378–383 (2009).
- ¹⁰⁷L. Liu, S. Li, X. N. He, X. Huang, C. F. Zhang, L. S. Fan, M. X. Wang, Y. S. Zhou, K. Chen, L. Jiang, J. F. Silvain, and Y. F. Lu, "Flame-enhanced laser-induced breakdown spectroscopy," *Opt. Express* **22**, 7686–7693 (2014).
- ¹⁰⁸Y. Liu, M. Baudalet, and M. Richardson, "Elemental analysis by microwave-assisted laser-induced breakdown spectroscopy: Evaluation on ceramics," *J. Anal. At. Spectrom.* **25**, 1316–1323 (2010).
- ¹⁰⁹M. Oba, M. Miyabe, K. Akaoka, and I. Wakaida, "Development of microwave-assisted, laser-induced breakdown spec-

- troscopy without a microwave cavity or waveguide,” *Japanese Journal of Applied Physics* **59**, 062001 (2020).
- ¹¹⁰Y. Ikeda and J. K. Soriano, “Microwave-enhanced laser-induced air plasma at atmospheric pressure,” *Opt. Express* **30**, 33756–33766 (2022).
- ¹¹¹Z. Yu, S. Yao, L. Zhang, Z. Lu, Z. S. Lie, and J. Lu, “Surface-enhanced laser-induced breakdown spectroscopy utilizing metallic target for direct analysis of particle flow,” *J. Anal. At. Spectrom.* **34**, 172–179 (2019).
- ¹¹²X. Yang, X. Li, Z. Cui, G. Yao, Z. Zhou, and K. Li, “Improving the sensitivity of surface-enhanced laser-induced breakdown spectroscopy by repeating sample preparation,” *Frontiers in Physics* **8** (2020), 10.3389/fphy.2020.00194, cited By 5.
- ¹¹³I. Elhandaoui, N. Mohamed, S. Selmani, P. Bouchard, M. Sababi, M. Constantin, and F. Vidal, “Rapid quantitative analysis of palladium in ores using laser-induced breakdown spectroscopy assisted with laser-induced fluorescence (libs-lif),” *J. Anal. At. Spectrom.*, – (2022).
- ¹¹⁴R. Zhou, K. Liu, Z. Tang, P. Gao, J. Yan, and X. Li, “High-sensitivity determination of available cobalt in soil using laser-induced breakdown spectroscopy assisted with laser-induced fluorescence,” *Appl. Opt.* **60**, 9062–9066 (2021).
- ¹¹⁵A. De Giacomo, R. Gaudiuso, C. Koral, M. Dell’Aglia, and O. De Pascale, “Nanoparticle enhanced laser induced breakdown spectroscopy: Effect of nanoparticles deposited on sample surface on laser ablation and plasma emission,” *Spectrochimica Acta Part B: Atomic Spectroscopy* **98**, 19–27 (2014).
- ¹¹⁶Z. Tang, K. Liu, Z. Hao, K. Liu, W. Zhang, Q. Li, C. Zhu, J. Chen, and X. Li, “The validity of nanoparticle enhanced molecular laser-induced breakdown spectroscopy,” *J. Anal. At. Spectrom.* **36**, 1034–1040 (2021).
- ¹¹⁷F. J. Fortes, A. Fernández-Bravo, and J. Javier Laserna, “Chemical characterization of single micro- and nano-particles by optical catapulting–optical trapping–laser-induced breakdown spectroscopy,” *Spectrochimica Acta Part B: Atomic Spectroscopy* **100**, 78–85 (2014), dedicated To Nicolo Omenetto On the Occasion of his 75th Birthday.
- ¹¹⁸P. Purohit, F. J. Fortes, and J. J. Laserna, “Optical trapping as a morphologically selective tool for in situ libs elemental characterization of single nanoparticles generated by laser ablation of bulk targets in air,” *Analytical Chemistry* **93**, 2635–2643 (2021), pMID: 33400487, <https://doi.org/10.1021/acs.analchem.0c04827>.
- ¹¹⁹P. Purohit, F. J. Fortes, and J. J. Laserna, “Atomization efficiency and photon yield in laser-induced breakdown spectroscopy analysis of single nanoparticles in an optical trap,” *Spectrochimica Acta Part B: Atomic Spectroscopy* **130**, 75–81 (2017).
- ¹²⁰G. A. Wubetu, H. Fiedorowicz, J. T. Costello, and T. J. Kelly, “Time resolved anisotropic emission from an aluminium laser produced plasma,” *Physics of Plasmas* **24**, 013105 (2017), <https://doi.org/10.1063/1.4973444>.
- ¹²¹M. Aghababaei Nejad, M. Soltanolkotabi, and A. Eslami Majd, “Polarization investigation of laser-induced breakdown plasma emission from al, cu, mo, w, and pb elements using nongated detector,” *Journal of Laser Applications* **30**, 022005 (2018), <https://doi.org/10.2351/1.5012507>.
- ¹²²G. A. Wubetu, T. J. Kelly, P. Hayden, H. Fiedorowicz, W. Skrzeczanowski, and J. T. Costello, “Recombination contributions to the anisotropic emission from a laser produced copper plasma,” *Journal of Physics B: Atomic, Molecular and Optical Physics* **53**, 065701 (2020).
- ¹²³A. Sharma and R. Thareja, “Anisotropic emission in laser-produced aluminum plasma in ambient nitrogen,” *Applied Surface Science* **253**, 3113–3121 (2007).
- ¹²⁴D. Zhao, N. Farid, R. Hai, D. Wu, and H. Ding, “Diagnostics of first wall materials in a magnetically confined fusion device by polarization-resolved laser-induced breakdown spectroscopy,” *Plasma Science and Technology* **16**, 149–154 (2014).
- ¹²⁵G. A. Wubetu, H. Fiedorowicz, J. T. Costello, and T. J. Kelly, “Time resolved anisotropic emission from an aluminium laser produced plasma,” *Physics of Plasmas* **24**, 013105 (2017), <https://doi.org/10.1063/1.4973444>.
- ¹²⁶K. Rifai, F. Vidal, M. Chaker, and M. Sababi, “Resonant laser-induced breakdown spectroscopy (libs) analysis of traces through selective excitation of aluminum in aluminum alloys,” *J. Anal. At. Spectrom.* **28**, 388–395 (2013).
- ¹²⁷K. Liu, Z. Tang, R. Zhou, W. Zhang, Q. Li, C. Zhu, C. He, K. Liu, and X. Li, “Determination of lead in aqueous solutions using resonant surface-enhanced libs,” *J. Anal. At. Spectrom.* **36**, 2480–2484 (2021).
- ¹²⁸M. Abdel-Harith, A. Elhassan, Z. Abdel-Salam, and M. F. Ali, “Back-reflection-enhanced laser-induced breakdown spectroscopy (brelibs) on transparent materials: Application on archaeological glass,” *Analytica Chimica Acta* **1184**, 339024 (2021).
- ¹²⁹S. Sharma, A. Misra, P. Lucey, R. Wiens, and S. Clegg, “Combined remote libs and raman spectroscopy at 8.6m of sulfur-containing minerals, and minerals coated with hematite or covered with basaltic dust,” *Spectrochimica Acta Part A: Molecular and Biomolecular Spectroscopy* **68**, 1036–1045 (2007), seventh International Conference on Raman Spectroscopy Applied to the Earth and Planetary Sciences.
- ¹³⁰S. M. Clegg, R. Wiens, A. K. Misra, S. K. Sharma, J. Lambert, S. Bender, R. Newell, K. Nowak-Lovato, S. Smrekar, M. D. Dyar, and S. Maurice, “Planetary geochemical investigations using raman and laser-induced breakdown spectroscopy,” *Applied Spectroscopy* **68**, 925–936 (2014), pMID: 25226246, <https://doi.org/10.1366/13-07386>.
- ¹³¹Q. Lin, G. Niu, Q. Wang, Q. Yu, and Y. Duan, “Combined laser-induced breakdown with raman spectroscopy: Historical technology development and recent applications,” *Applied Spectroscopy Reviews* **48**, 487–508 (2013), <https://doi.org/10.1080/05704928.2012.751028>.
- ¹³²D. V. S, S. D. George, V. B. Kartha, S. Chidangil, and U. V. K, “Hybrid libs-raman-lif systems for multi-modal spectroscopic applications: a topical review,” *Applied Spectroscopy Reviews* **56**, 463–491 (2021), <https://doi.org/10.1080/05704928.2020.1800486>.
- ¹³³V. N. Lednev, S. M. Pershin, P. A. Sdvizhenskii, M. Y. Grishin, A. N. Fedorov, V. V. Bukin, V. B. Oshurko, and A. N. Shchegolikhin, “Combining raman and laser induced breakdown spectroscopy by double pulse lasing,” *Analytical and Bioanalytical Chemistry* **410**, 277–286 (2018).
- ¹³⁴K. Muhammed Shameem, V. Dhanada, S. D. George, V. Kartha, C. Santhosh, and V. Unnikrishnan, “Assessing the feasibility of a low-throughput gated echelle spectrograph for laser-induced breakdown spectroscopy (libs)-raman measurements at standoff distances,” *Optics & Laser Technology* **153**, 108264 (2022).
- ¹³⁵K. Meissner, T. Lippert, A. Wokaun, and D. Guenther, “Analysis of trace metals in comparison of laser-induced breakdown spectroscopy with la-icp-ms,” *Thin Solid Films* **453-454**, 316–322 (2004), proceedings of Symposium H on Photonic Processing of Surfaces, Thin Films and Devices, of the E-MRS 2003 Spring Conference.
- ¹³⁶D. Oropeza, J. González, J. Chirinos, V. Zorba, E. Rogel, C. Ovalles, and F. López-Linares, “Elemental analysis of asphaltenes using simultaneous laser-induced breakdown spectroscopy (libs)–laser ablation inductively coupled plasma optical emission spectrometry (la-icp-oes),” *Appl. Spectrosc.* **73**, 540–549 (2019).
- ¹³⁷J. R. Chirinos, D. D. Oropeza, J. J. Gonzalez, H. Hou, M. Morey, V. Zorba, and R. E. Russo, “Simultaneous 3-dimensional elemental imaging with libs and la-icp-ms,” *J. Anal. At. Spectrom.* **29**, 1292–1298 (2014).
- ¹³⁸L. Brunnbauer, M. Mayr, S. Larisegger, M. Nelhiebel, L. Pagnin, R. Wiesinger, M. Schreiner, and A. Limbeck, “Combined la-icp-ms/libs: powerful analytical tools for the investigation of

polymer alteration after treatment under corrosive conditions,” [Scientific Reports](#) **10**, 12513 (2020).

¹³⁹M. F. Alberghina, R. Barraco, M. Brai, T. Schillaci, and L. Tranchina, “Double laser LIBS and micro-XRF spectroscopy applied to characterize materials coming from the Greek-Roman theater of Taormina,” in [O3A: Optics for Arts, Architecture, and Archaeology II](#), Vol.

7391, edited by L. Pezzati and R. Salimbeni, International Society for Optics and Photonics (SPIE, 2009) p. 739107.

¹⁴⁰A. P. Rao, P. R. Jenkins, J. D. Auxier, M. B. Shattan, and A. K. Patnaik, “Analytical comparisons of handheld libs and xrf devices for rapid quantification of gallium in a plutonium surrogate matrix,” [J. Anal. At. Spectrom.](#) **37**, 1090–1098 (2022).